J Seismol (2017) 21:99–125
DOI 10.1007/s10950-016-9586-4

ORIGINAL ARTICLE

Ground motion prediction equations for horizontal and vertical components of acceleration in Northern Iran

M. R. Soghrat · M. Ziyaeifar

Received: 4 May 2015 / Accepted: 16 May 2016 / Published online: 25 May 2016

Abstract Recent studies have shown that the vertical component of ground motion can be quite destructive on a variety of structural systems. Development of response spectrum for design of buildings subjected to vertical component of earthquake needs ground motion prediction equations (GMPEs). The existing GMPEs for northern Iranian plateau are proposed for the horizontal component of earthquake, and there is not any specified GMPE for the vertical component of earthquake in this region. Determination of GMPEs is mostly based on regression analyses on earthquake parameters such as magnitude, site class, distance, and spectral amplitudes. In this study, 325 three-component records of 55 earthquakes with magnitude ranging from M_w 4.1 to M_w 7.3 are used for estimation on the regression coefficients. Records with distances less than 300 km are selected for analyses in the database. The regression analyses on earthquake parameters results in determination of GMPEs for peak ground acceleration and spectral acceleration for both horizontal and vertical components of the ground motion. The correlation between the models for vertical and horizontal GMPEs is studied in details. These models are later compared with some other available GMPEs. According to the result of this investigation, the proposed GMPEs are in agreement with the other relationships that were developed based on the local and regional data.

Keywords Ground motion prediction equations · Horizontal and vertical component of earthquake · Peak ground acceleration · Spectral acceleration · Iran

M. R. Soghrat (✉) · M. Ziyaeifar
International Institute of Earthquake Engineering and Seismology (IIEES), No. 26, Arghavan St., North Dibajee, Farmanieh, P.O. Box: 19395/3913, Tehran, Iran
e-mail: m.soghrat@iiees.ac.ir

1 Introduction

In last two decades, some great earthquakes (e.g., Kobe 1995, Chi-chi 1999, and Bam 2003) have shown the importance of vertical component of earthquake in inflicting damage on a variety of structural systems (e.g., Palaskas et al. 1996). Saadeghvaziri and Foutch (1991) have shown that axial load variation in columns due to vertical excitation can even cause instability in certain type of structural systems. Yu et al. (1997) have reported about 21 % increase in axial load of columns and about 7 % variation in their moments. In another work, however, Shakib and Fuladgar (2003) have studied a base isolated structure subjected to vertical and horizontal component of earthquake in which axial load in columns of the studied structures was up to three times of what it was expected (without considering the vertical component of the earthquakes). Generally, it is believed that the effects of vertical component of earthquake in structural responses are more pronounced in the near fault regions (e.g., Button et al. 2002; Kunnath et al. 2008; Bommer et al. 2011; Gülerce and Abrahamson 2011).

According to above results, it seems that, in the structural design procedure, both horizontal and vertical design spectra are required in the process to reduce the vulnerability of the structural systems to seismic hazards. However, some of the existing design codes/guidelines are providing the designers only with the horizontal spectrum (such as Standard 2800 2014, Iranian code of practice for seismic restraint design of buildings). In some others, the vertical spectrum is defined using a ratio of 2/3 with respect to the horizontal one (e.g., FEMA 356 2000; ASCE 41 2013). The new trend is toward introducing vertical spectrum using vertical-to-horizontal spectral ratios (such as Eurocode 8 2004; FEMA P-750 2009). Vertical spectrum in Eurocode 8 (2004) is partially based on the model proposed by Elnashai and Papazoglou (1997) and the one introduced in FEMA P-750 (2009) is on the basis of the methodology developed by Bozorgnia and Campbell (2004). Elnashai and Papazoglou (1997) introduced the vertical design spectrum with a flat plateau at short periods (0.05–0.15 s). Bozorgnia and Campbell (2004) proposed a simplified vertical to horizontal spectral ratio (V/H) for scaling the horizontal spectrum to the vertical one.

Typically, there are two different approaches in obtaining the vertical component of response spectrum using ground motion prediction equations (GMPEs). The differences between these approaches are based on the method of using GMPEs in development of vertical spectrum. The first approach is a direct application of GMPEs for vertical component of earthquake, and in the second one, the attenuation model is in the form of vertical to horizontal spectral ratio function. The attenuation model in this case will be used to scale the horizontal spectrum to the vertical one (Ambraseys and Douglas 2003; Bommer et al. 2011; Gülerce and Abrahamson 2011; Soghrat and Ziyaeifar 2016). While V/H ratio usually scales down the horizontal spectrum, it may scale up the spectrum in near distances particularly for the short period range of the response spectrum.

GMPEs have a key role in seismic hazard evaluation for site-specific spectra. To propose a GMPE for any specific region, the magnitude, source-to-site distance, and peak ground characteristics of the earthquakes in that region are required. In addition, some other parameters such as site class, faulting mechanism, and so on might be considered necessary in development of GMPEs for a particular region. GMPEs can be developed using physical or mathematical approaches. For the regions with limited records of ground motion, the application of physical models will be essential for successful prediction of ground motions. In this approach, limited records are employed for the physical model calibration. These models usually have been developed in the context of the random vibration theory and the stochastic modeling approach (see, e.g., Halldorsson and Papageorgiou 2005; Soghrat et al. 2012). One of the most remarkable advantages of physical models relative to mathematical models is that source, path, and site effects may be derived from available limited data through calibration of physical models (in this approach, using ground motion records in back-calculation studies results in finding the ground motion unknown parameters and leads to development of the GMPEs).

Mathematical method, based on regression analyses, is used when abundant records of ground motion are available for the studied region. For regions where there are sufficient data, these mathematical methods are suitable and have been successfully developed. Data sufficiency, type of regression technique, and the classification of data are effective in validity and accuracy of these methods (Soghrat et al. 2012).

Although, various GMPEs have been developed for horizontal component of earthquake in the region (using both physical and mathematical approaches as reported by Sinaiean 2006; Ghodrati-Amiri et al. 2009; Ghasemi et al. 2009; Soghrat et al. 2012; Zafarani and Soghrat 2012), there are no reliable GMPEs for vertical component of earthquake in northern Iran or the whole Iranian plateau based on the recorded data in this large area.

In the current work, using a mathematical approach based on the recorded data and events in the studied region, a database consisting of selected records and events is developed. Among the available functional form for the GMPEs, the one that shows a better fitness to the local data is chosen. Later, the regression coefficients for both horizontal and vertical GMPEs were determined independently. After evaluating the integrity of results, a comparison with some other studies has been carried out to show the accuracy of the models proposed in this work.

2 Database and record processing

Iranian plateau is considered as a large earthquake prone zone, and it is divided into five different tectonic regions (Azerbaijan-Alborz, Kopeh Dagh, Zagros, Makran and central–east Iran classified by Mirzaei et al. 1998). These regions are all shown in Fig. 1. In this work, northern Iran including Azerbaijan-Alborz and Kope-Dagh regions are considered for further studies.

The strong motion data for these regions has been recorded by the Iranian Strong Motion Network (ISMN) that can be accessed through the Building and Housing Research Center (BHRC). This network consists of more than 1100 stations and has more than 10,000 three-component accelerograms (analog and digital recordings) in various active seismic regions of the country.

For reducing uncertainties, only those records with available average S-wave velocity in the depth of 30 m (V_{s30}) are chosen from the database. Four site groups in terms of Vs30 have been adopted in this study (I, $V_{s30} > 750$; II, $375 < V_{s30} < 750$; III, $175 < V_{s30} < 375$; and IV, $V_{s30} < 175$). This classification is based on the Standard 2800 (2014) (Iranian Code of Practice for Seismic Resistant design of Building) which is similar to the one proposed by Eurocode 8 (2004) (A, Vs30 > 800; B, 360 < Vs30 < 800; C, 180 < Vs30 < 360; and D, Vs30 < 180). Altogether, 325 acceleration time histories (listed in Appendix Table 7) from 55 earthquakes (tabulated in Table 1) are used in the database. According to this dataset, site classifications for both standards (2800 and Eurocode) are the same for 98 % of the records (318 of 325 records).

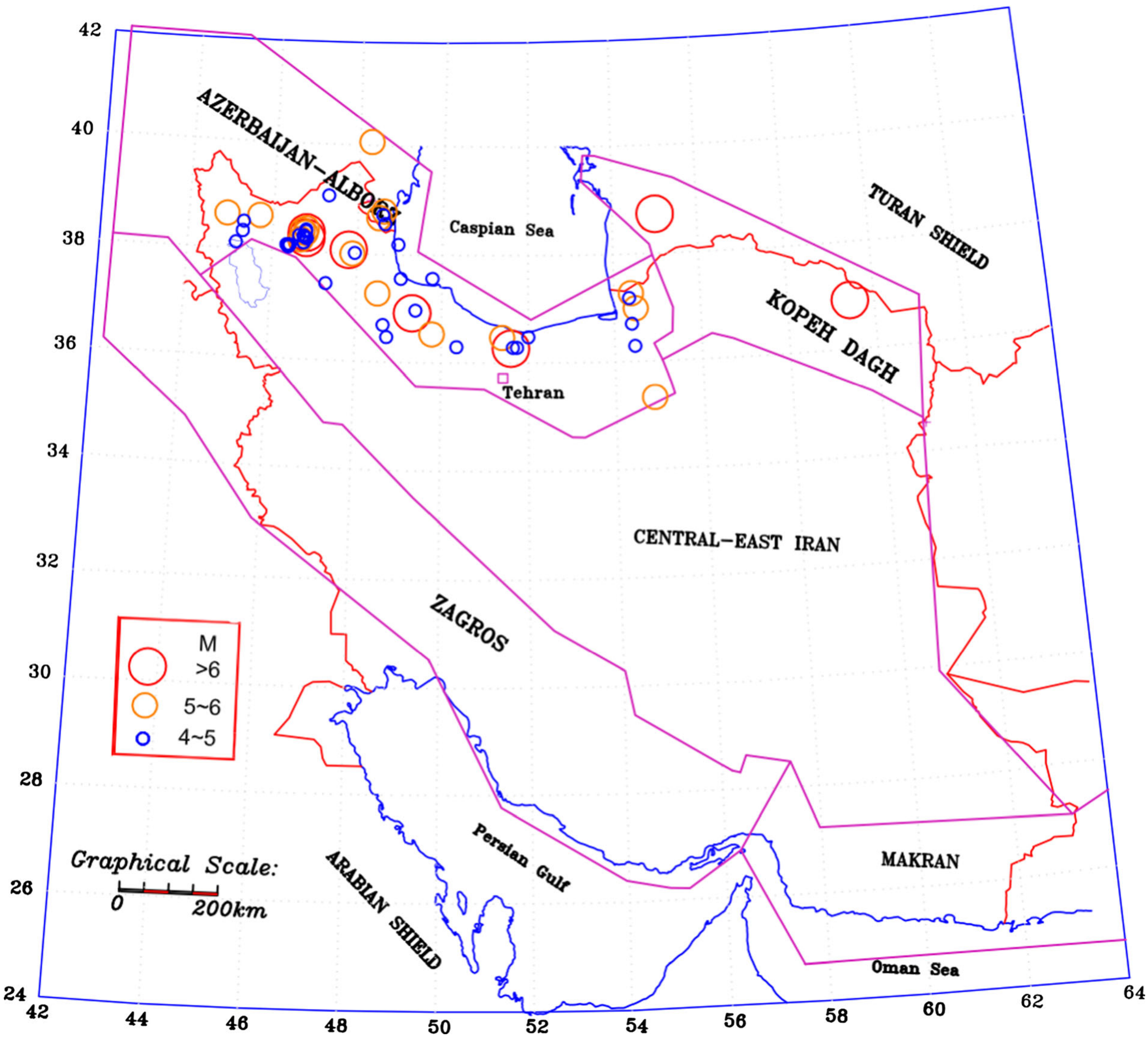

Fig. 1 Five tectonic regions of Iran (Mirzaei et al. 1998) and distribution of the studied earthquakes

Table 1 The list of earthquakes used in analyses procedure

No.	Date	Time	Lat_epi	Lon_epi	Depth	Final M_w	*SF*	*N*
1	June 20, 1990	21:00:11	36.96	49.33	12.0	7.3	SS	2
2	February 4, 1997	10:37:47	37.39	57.35	8.0	6.4	SS	3
3	February 28, 1997	12:57:45	38.10	47.79	9.0	6	SS	12
4	March 2, 1997	18:29:42	38.00	47.89	10.0	5.3	RV	2
5	March 21, 1997	23:00:39	38.01	47.87	10.0	4.9	U	2
6	July 9, 1998	14:19:18	38.71	48.50	27.0	5.7	RV	14
7	July 9, 1998	16:23:35	38.73	48.64	9.9	4.6	U	4
8	September 28, 1998	17:26:30	36.51	48.72	15.0	4.5	U	9
9	November 23, 1998	11:11:38	38.32	45.15	18.7	4.9	U	3
10	March 26, 1999	12:06:53	36.33	50.27	7.0	4.5	U	3
11	November 19, 1999	4:40:24	37.30	54.39	26.0	5.4	RV	9
12	November 26, 1999	4:27:24	36.95	54.89	10.0	5.3	RV	4
13	March 21, 2000	14:07:38	40.03	48.22	57.8	5.1	SS	3
14	March 9, 2000	19:02:55	37.40	47.28	5.0	4.1	U	3
15	August 16, 2000	12:53:01	36.72	54.37	25.0	4.9	RV	3
16	December 6, 2000	17:11:05	38.53	54.80	31.0	7	RV	3
17	June 12, 2001	1:46:49	39.10	47.28	15.0	4.5	RV	2
18	January 5, 2002	14:43:42	37.58	49.00	27.3	4.7	SS	5
19	January 6, 2002	6:22:27	38.25	48.95	9.7	4.3	U	2
20	February 14, 2002	20:06:23	36.98	49.42	15.0	4.4	SS	3
21	April 8, 2002	18:30:58	36.46	52.01	8.5	4.9	RV	2
22	April 19, 2002	13:46:49	36.55	49.74	33.6	5.2	RV	11
23	August 11, 2003	20:12:08	38.72	44.92	7.6	5.2	SS	3
24	May 28, 2004	12:38:44	36.28	51.58	17.0	6.3	RV	49
25	May 29, 2004	9:23:48	36.49	51.37	7.5	5	RV	4
26	May 30, 2004	1:42:43	36.33	51.65	11.0	4.6	U	2
27	May 30, 2004	19:27:01	36.38	51.66	8.5	4.6	U	2
28	September 5, 2004	17:33:58	38.56	45.32	9.7	4.3	U	4
29	October 8, 2004	13:45:55	37.17	54.35	31.0	4.8	U	2
30	January 10, 2005	18:47:30	37.06	54.53	29.0	5.2	RV	15
31	November 29, 2005	5:57:03	37.37	54.46	27.0	4.9	U	2
32	November 5, 2006	20:06:40	37.40	48.80	20.0	4.8	SS	4
33	September 11, 2007	6:51:12	38.79	48.60	25.0	5.2	U	12
34	September 16, 2007	5:20:01	38.10	46.38	15.6	4.1	U	2
35	December 1, 2007	18:22:17	38.07	46.40	5.0	4.4	U	2
36	December 1, 2007	18:45:11	38.09	46.43	7.4	4.7	U	3
37	December 2, 2007	10:00:02	38.06	46.40	7.9	4.3	U	2
38	March 23, 2008	12:11:31	37.31	48.51	6.0	5.1	U	2
39	May 27, 2008	6:18:08	36.65	48.66	23.0	4.8	U	5
40	September 2, 2008	20:00:56	38.68	45.74	10.7	5	SS	5
41	August 11, 2012	12:23:15	38.31	46.80	7.0	6.4	SS	22
42	August 11, 2012	12:34:34	38.39	46.81	19.2	6.4	RV	37
43	August 11, 2012	12:30:12	38.41	46.79	6.1	4.6	U	5
44	August 11, 2012	12:49:14	38.40	46.69	4.5	4.8	U	2

Table 1 (continued)

No.	Date	Time	Lat_epi	Lon_epi	Depth	Final M_w	*SF*	*N*
45	August 11, 2012	15:21:14	38.43	46.80	4.0	4.7	U	4
46	August 11, 2012	15:43:19	38.46	46.74	7.4	4.7	U	4
47	August 11, 2012	22:24:02	38.35	46.73	4.0	5.2	U	5
48	August 13, 2012	1:56:10	38.42	46.69	4.0	4.6	U	2
49	August 14, 2012	14:02:25	38.50	46.81	7.4	5	U	6
50	August 15, 2012	17:49:04	38.44	46.67	4.0	5	RV	3
51	August 16, 2012	17:14:12	38.46	46.73	4.0	4.6	U	2
52	August 19, 2012	1:58:29	38.41	46.66	4.0	4.5	U	2
53	September 27, 2012	0:56:00	38.42	46.63	4.0	4.6	U	2
54	October 26, 2012	22:31:16	38.46	46.65	10.0	4.5	U	2
55	November 7, 2012	6:26:31	38.45	46.52	10.0	5.6	SS	3

SF style of faulting, *RV* reverse, *SS* strike-slip, *U* unknown, *N* number of records

The range of moment magnitude (M_w) of these events is about 4.1–7.3. Figure 1 shows the locations of the epicenters of these earthquakes. It should be noted that, the moment magnitude of 10 earthquakes (the event number of 5, 7, 9, 10, 19, 35, 36, 37, 38 and 54 in Table 1) with 26 records (about 20 % of events and 8 % of records) are estimated from the magnitude conversion relations reported by Shahvar et al. (2013).

The magnitude-distance distribution for these events is illustrated in Fig. 2. According to this figure, the database is well suited for the records with the magnitudes of 6.5 and lower (and distances less than 200 km). Since the epicentral distance for all the records are available in the dataset, if the Joyner-Boore distance (Rjb) is not available, the epicentral distance is used instead. It should be mentioned that, for the earthquakes with $M_w \geq 6$, the Joyner-Boore distance is available for all cases.

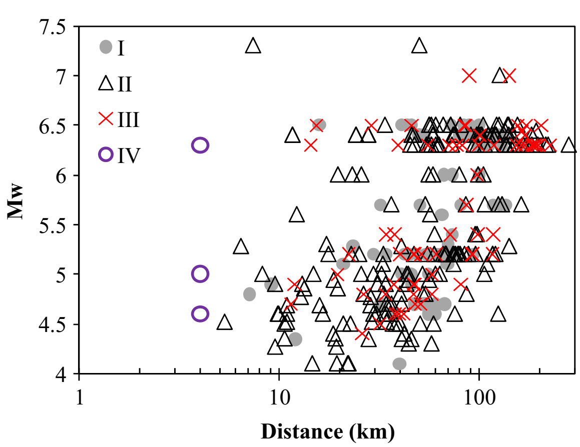

Fig. 2 Distribution of moment magnitude-distance versus site classification (Standard 2800 2014)

Histograms for the number of records versus distance and magnitude are shown in Fig. 3. According to these histograms, the dataset is dominated by the records with distances of 50–100 km (about 35 % of records) as well as by those with the moment magnitude of 6–6.5 (about 38 % records).

In about 52 % of the events, there is no information (NA) about their faulting mechanisms in the studied region (attributed to the events with $M_w \leq 5.2$). The events with reverse and strike-slip faulting are representing about 27 and 21 % of the incidents, respectively. From the viewpoint of record frequency, about 50 % of the records are considered reverse faulting, 20 % are strike-slip faulting and the rest are assumed as unknown.

To reduce the uncertainty in results, the records with the following features are omitted from the dataset: data from instruments that triggered during the S-wave train; stations with no information on the site conditions; data with poor quality; records with only a single horizontal component; and the events that recorded by only one station.

The uncorrected (unprocessed) acceleration time series were corrected by a new multiresolution wavelet analysis proposed by Ansari et al. (2010) to remove undesirable noise from the recorded signals.

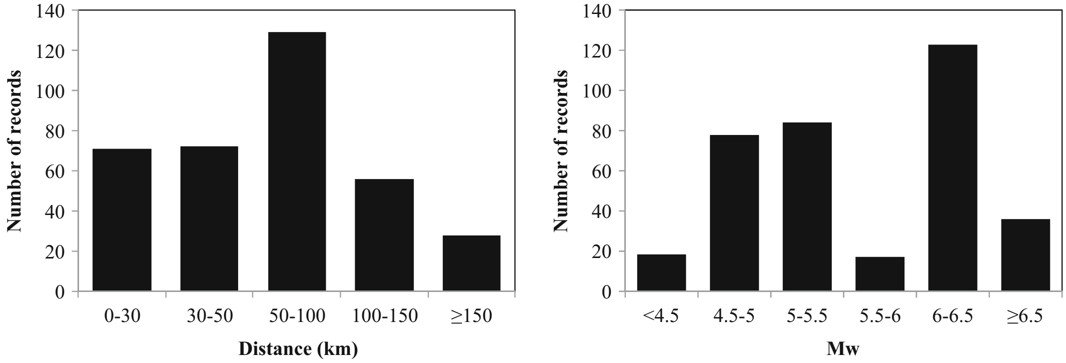

Fig. 3 Histograms of records versus distance and magnitude

Table 2 Regression coefficients for horizontal GMPE in model 1

T	*b*1	*b*2	*b*3	*b*4	*b*5	*b*6	*S*1	*S*2	*S*3	*S*4*b*	*fs*	*frv*	*fuu*	*σ*	*τ*
0	−2.237	1.695	−0.131	−1.407	0.063	7.5	0.250	0.221	0.281	−0.021	−0.137	−0.124	−0.008	0.028	0.259
0.01	−2.249	1.697	−0.131	−1.396	0.061	7.5	0.252	0.222	0.282	−0.021	−0.135	−0.122	−0.007	0.028	0.259
0.02	−2.316	1.724	−0.132	−1.363	0.053	7.5	0.247	0.216	0.275	−0.031	−0.144	−0.131	−0.017	0.028	0.261
0.03	−2.231	1.713	−0.132	−1.422	0.057	7.5	0.280	0.233	0.295	−0.027	−0.121	−0.105	0.007	0.028	0.261
0.04	−2.076	1.655	−0.126	−1.428	0.051	7.5	0.339	0.277	0.334	−0.001	−0.062	−0.046	0.057	0.029	0.265
0.05	−1.945	1.636	−0.125	−1.451	0.047	7.5	0.368	0.290	0.344	0.001	−0.046	−0.027	0.077	0.029	0.267
0.07	−1.650	1.547	−0.122	−1.567	0.063	7.5	0.490	0.381	0.424	0.108	0.094	0.107	0.201	0.029	0.267
0.1	−2.239	1.994	−0.166	−1.750	0.093	7.5	0.336	0.213	0.242	−0.046	−0.139	−0.117	0.001	0.030	0.274
0.15	−1.167	1.587	−0.147	−2.565	0.245	7.5	0.563	0.507	0.542	0.221	0.247	0.234	0.352	0.107	0.280
0.2	−1.291	1.582	−0.147	−2.435	0.213	7.5	0.462	0.464	0.526	0.257	0.214	0.193	0.303	0.105	0.276
0.25	−1.691	1.600	−0.135	−1.887	0.157	7.5	0.279	0.360	0.436	0.234	0.064	0.082	0.163	0.098	0.289
0.3	−1.823	1.601	−0.131	−1.831	0.152	7.5	0.187	0.330	0.410	0.251	0.022	0.040	0.115	0.111	0.292
0.35	−2.000	1.548	−0.117	−1.514	0.101	7.5	0.095	0.292	0.393	0.220	−0.030	−0.007	0.037	0.122	0.290
0.4	−2.294	1.624	−0.120	−1.457	0.052	7.5	0.008	0.220	0.334	0.144	−0.135	−0.103	−0.057	0.123	0.294
0.45	−2.697	1.716	−0.119	−1.160	0.052	7.5	−0.108	0.115	0.221	0.075	−0.286	−0.228	−0.183	0.133	0.292
0.5	−2.773	1.653	−0.106	−0.979	0.022	7.5	−0.122	0.095	0.194	0.059	−0.315	−0.251	−0.208	0.131	0.288
0.6	−3.159	1.823	−0.121	−1.155	0.056	7.5	−0.235	0.006	0.118	−0.048	−0.419	−0.400	−0.341	0.140	0.286
0.7	−3.256	1.911	−0.136	−1.530	0.125	7.5	−0.259	−0.024	0.089	−0.062	−0.438	−0.444	−0.374	0.150	0.285
0.75	−3.254	1.875	−0.132	−1.537	0.131	7.5	−0.262	−0.026	0.081	−0.047	−0.442	−0.433	−0.379	0.141	0.288
0.8	−3.408	1.901	−0.129	−1.440	0.113	7.5	−0.299	−0.062	0.050	−0.097	−0.504	−0.478	−0.427	0.142	0.290
0.9	−3.399	1.882	−0.130	−1.573	0.138	7.5	−0.295	−0.063	0.054	−0.095	−0.500	−0.467	−0.431	0.144	0.293
1	−3.652	2.021	−0.143	−1.730	0.165	7.5	−0.348	−0.123	−0.022	−0.159	−0.570	−0.554	−0.528	0.156	0.297
1.2	−4.114	2.226	−0.162	−1.821	0.183	7.5	−0.458	−0.235	−0.118	−0.302	−0.698	−0.715	−0.701	0.178	0.300
1.4	−4.093	2.102	−0.145	−1.673	0.160	7.5	−0.470	−0.243	−0.100	−0.280	−0.662	−0.711	−0.720	0.191	0.305
1.5	−3.986	2.024	−0.138	−1.723	0.170	7.5	−0.453	−0.226	−0.083	−0.224	−0.625	−0.678	−0.683	0.193	0.307
1.6	−3.943	1.943	−0.127	−1.648	0.155	7.5	−0.442	−0.206	−0.069	−0.225	−0.615	−0.664	−0.664	0.183	0.308
1.8	−3.719	1.774	−0.109	−1.681	0.156	7.5	−0.392	−0.161	−0.015	−0.151	−0.538	−0.590	−0.590	0.183	0.309
2	−3.582	1.563	−0.082	−1.445	0.116	7.5	−0.345	−0.131	0.029	−0.134	−0.502	−0.544	−0.537	0.173	0.310
2.5	−2.964	1.085	−0.035	−1.318	0.098	7.5	−0.178	−0.003	0.147	0.069	−0.292	−0.335	−0.338	0.167	0.299
3	−2.421	0.723	−0.004	−1.367	0.108	7.5	−0.032	0.126	0.271	0.214	−0.102	−0.152	−0.167	0.158	0.282
4	−1.681	0.266	0.031	−1.456	0.127	7.5	0.174	0.318	0.444	0.383	0.177	0.078	0.064	0.167	0.253

Table 3 Regression coefficients for vertical GMPE in model 1

T	*b*1	*b*2	*b*3	b4	*b*5	*b*6	*S*1	*S*2	*S*3	*S4b*	*fs*	*frv*	*fuu*	*σ*	*τ*
0	−0.357	0.639	−0.045	−1.733	0.105	7.5	0.771	0.744	0.746	0.382	0.527	0.523	0.594	0.052	0.271
0.01	−0.356	0.635	−0.044	−1.705	0.099	7.5	0.774	0.745	0.747	0.378	0.528	0.523	0.592	0.069	0.276
0.02	−0.402	0.689	−0.048	−1.738	0.099	7.5	0.766	0.735	0.733	0.365	0.517	0.509	0.572	0.069	0.285
0.03	−0.268	0.684	−0.046	−1.771	0.085	7.5	0.820	0.768	0.775	0.368	0.579	0.553	0.600	0.094	0.277
0.04	−0.273	0.767	−0.053	−1.863	0.084	7.5	0.847	0.759	0.760	0.361	0.582	0.543	0.602	0.097	0.285
0.05	−0.110	0.757	−0.057	−2.051	0.113	7.5	0.881	0.803	0.784	0.422	0.637	0.600	0.652	0.097	0.284
0.07	−0.370	0.903	−0.066	−2.027	0.110	7.5	0.806	0.725	0.698	0.402	0.510	0.484	0.636	0.099	0.290
0.1	−0.077	0.796	−0.069	−2.300	0.188	7.5	0.881	0.784	0.785	0.472	0.613	0.589	0.721	0.101	0.296
0.15	1.144	0.322	−0.054	−3.180	0.366	7.5	1.101	1.101	1.143	0.798	1.018	1.015	1.111	0.106	0.312
0.2	0.313	0.668	−0.078	−2.987	0.340	7.5	0.845	0.905	0.933	0.631	0.782	0.743	0.788	0.143	0.292
0.25	−0.527	0.867	−0.078	−2.314	0.237	7.5	0.565	0.691	0.707	0.510	0.469	0.456	0.548	0.122	0.290
0.3	−0.517	0.993	−0.104	−3.039	0.368	7.5	0.593	0.698	0.704	0.488	0.463	0.466	0.554	0.145	0.296
0.35	−1.447	1.110	−0.082	−1.862	0.164	7.5	0.347	0.473	0.477	0.257	0.155	0.171	0.228	0.129	0.284
0.4	−2.524	1.468	−0.093	−1.218	0.050	7.5	0.109	0.215	0.198	−0.045	−0.198	−0.192	−0.134	0.132	0.291
0.45	−2.805	1.617	−0.108	−1.380	0.082	7.5	0.029	0.154	0.097	−0.085	−0.319	−0.268	−0.218	0.133	0.293
0.5	−3.072	1.709	−0.113	−1.267	0.063	7.5	−0.060	0.085	0.011	−0.107	−0.387	−0.355	−0.329	0.135	0.296
0.6	−2.805	1.617	−0.108	−1.380	0.018	7.5	0.029	0.154	0.097	−0.085	−0.319	−0.268	−0.218	0.133	0.293
0.7	−3.898	1.899	−0.114	−0.803	0.001	7.5	−0.311	−0.171	−0.222	−0.195	−0.639	−0.640	−0.620	0.119	0.312
0.75	−3.978	1.923	−0.118	−0.881	0.022	7.5	−0.321	−0.184	−0.239	−0.234	−0.669	−0.666	−0.643	0.119	0.313
0.8	−4.343	2.092	−0.130	−0.822	0.012	7.5	−0.402	−0.266	−0.329	−0.346	−0.784	−0.783	−0.776	0.120	0.316
0.9	−4.527	2.154	−0.134	−0.842	0.012	7.5	−0.431	−0.310	−0.350	−0.436	−0.839	−0.850	−0.837	0.133	0.317
1	−4.558	2.149	−0.132	−0.904	0.021	7.5	−0.438	−0.330	−0.328	−0.463	−0.843	−0.857	−0.858	0.122	0.319
1.2	−4.197	1.861	−0.103	−0.887	0.021	7.5	−0.392	−0.294	−0.214	−0.297	−0.716	−0.720	−0.761	0.155	0.316
1.4	−4.566	2.000	−0.111	−0.814	0.006	7.5	−0.513	−0.410	−0.329	−0.315	−0.818	−0.858	−0.890	0.187	0.315
1.5	−4.542	1.985	−0.111	−0.882	0.018	7.5	−0.536	−0.410	−0.327	−0.270	−0.802	−0.848	−0.892	0.206	0.312
1.6	−4.644	2.034	−0.116	−0.927	0.025	7.5	−0.581	−0.431	−0.348	−0.284	−0.842	−0.880	−0.922	0.208	0.315
1.8	−4.165	1.665	−0.079	−0.823	0.009	7.5	−0.435	−0.273	−0.209	−0.249	−0.692	−0.715	−0.758	0.189	0.319
2	−3.580	1.300	−0.048	−0.916	0.029	7.5	−0.270	−0.122	−0.086	−0.102	−0.491	−0.521	−0.568	0.183	0.309
2.5	−2.044	0.321	0.037	−0.937	0.053	7.5	0.135	0.240	0.287	0.294	0.048	−0.022	−0.070	0.181	0.289
3	−1.693	0.044	0.065	−0.865	0.040	7.5	0.192	0.327	0.360	0.429	0.160	0.096	0.051	0.154	0.275
4	−0.946	−0.493	0.113	−0.657	0.015	7.5	0.347	0.489	0.533	0.686	0.435	0.332	0.287	0.131	0.267

3 Functional forms

The form of a ground motion model is usually a function of magnitude, distance, site class, and other available parameters (e.g., style of faulting). Several functional forms have been examined to find a reliable one with the least possible error to fit our dataset. Among different classes of functional forms for modeling the ground motion, the following one is selected for further studies. This functional form is similar to the one proposed by Akkar and Bommer (2007, 2010).

$$Log_{10}(Y) = b_1 + b_2 Mw + b_3 Mw^2 + (b_4 + b_5 Mw)\log_{10}\sqrt{R^2 + {b_6}^2} + S_i + f_s F_S + f_{rv} F_{RV} + f_{uu} F_U \quad (1)$$

where Y is the response variable (PGA and PSA in cm/s^2); Mw, the moment magnitude; and R is the distance. b_1 to b_6

Table 4 Regression coefficients for horizontal GMPE in model 2 using continuous Vs30

T	*b*1	*b*2	*b*3	*b*4	*b*5	*b*6		*fs*	*frv*	*fuu*	σ	τ
0	−2.093	1.702	−0.132	−1.389	0.064	7.5	0.013	−0.074	−0.061	0.043	0.028	0.263
0.01	−2.098	1.704	−0.132	−1.378	0.061	7.5	0.016	−0.077	−0.063	0.040	0.029	0.262
0.02	−2.155	1.729	−0.133	−1.344	0.053	7.5	0.023	−0.094	−0.081	0.021	0.028	0.262
0.03	−2.061	1.719	−0.133	−1.393	0.056	7.5	0.052	−0.065	−0.047	0.050	0.028	0.264
0.04	−1.865	1.659	−0.127	−1.392	0.049	7.5	0.091	0.003	0.022	0.110	0.028	0.268
0.05	−1.749	1.643	−0.126	−1.403	0.043	7.5	0.125	0.039	0.062	0.148	0.028	0.270
0.07	−1.372	1.561	−0.123	−1.508	0.057	7.5	0.186	0.173	0.191	0.265	0.028	0.270
0.1	−2.077	2.001	−0.167	−1.694	0.087	7.5	0.240	−0.079	−0.049	0.049	0.030	0.276
0.15	−0.840	1.580	−0.144	−2.422	0.223	7.5	0.112	0.358	0.349	0.454	0.107	0.281
0.2	−1.102	1.590	−0.143	−2.217	0.209	7.5	−0.069	0.280	0.258	0.359	0.105	0.276
0.25	−1.456	1.607	−0.136	−1.925	0.166	7.5	−0.258	0.148	0.157	0.239	0.098	0.289
0.3	−1.610	1.588	−0.130	−1.842	0.154	7.5	−0.376	0.099	0.105	0.186	0.111	0.292
0.35	−1.785	1.513	−0.114	−1.530	0.104	7.5	−0.483	0.049	0.058	0.109	0.122	0.291
0.4	−2.317	1.588	−0.109	−1.186	0.054	7.5	−0.528	−0.136	−0.116	−0.065	0.124	0.295
0.45	−2.598	1.666	−0.114	−1.173	0.055	7.5	−0.542	−0.248	−0.202	−0.148	0.123	0.293
0.5	−2.710	1.619	−0.104	−1.010	0.027	7.5	−0.538	−0.286	−0.238	−0.186	0.131	0.288
0.6	−3.138	1.753	−0.114	−1.118	0.050	7.5	−0.563	−0.406	−0.399	−0.332	0.132	0.288
0.7	−3.240	1.840	−0.128	−1.513	0.123	7.5	−0.547	−0.427	−0.444	−0.368	0.141	0.288
0.75	−3.247	1.810	−0.125	−1.520	0.128	7.5	−0.538	−0.434	−0.437	−0.376	0.142	0.290
0.8	−3.427	1.835	−0.123	−1.425	0.110	7.5	−0.545	−0.503	−0.490	−0.434	0.144	0.292
0.9	−3.440	1.829	−0.124	−1.565	0.136	7.5	−0.560	−0.507	−0.488	−0.446	0.144	0.294
1	−3.775	1.979	−0.138	−1.702	0.160	7.5	−0.556	−0.603	−0.603	−0.569	0.156	0.297
1.2	−4.316	2.187	−0.157	−1.815	0.183	7.5	−0.575	−0.755	−0.790	−0.770	0.177	0.300
1.4	−4.290	2.070	−0.142	−1.705	0.166	7.5	−0.617	−0.717	−0.784	−0.789	0.191	0.304
1.5	−4.185	1.998	−0.136	−1.757	0.176	7.5	−0.633	−0.680	−0.753	−0.752	0.192	0.306
1.6	−4.114	1.908	−0.124	−1.675	0.160	7.5	−0.637	−0.660	−0.730	−0.724	0.191	0.305
1.8	−3.879	1.749	−0.107	−1.706	0.161	7.5	−0.638	−0.581	−0.651	−0.646	0.182	0.308
2	−3.746	1.557	−0.082	−1.483	0.124	7.5	−0.635	−0.546	−0.606	−0.595	0.172	0.308
2.5	−3.073	1.110	−0.039	−1.371	0.108	7.5	−0.583	−0.318	−0.378	−0.377	0.165	0.296
3	−2.444	0.758	−0.008	−1.423	0.118	7.5	−0.552	−0.100	−0.166	−0.178	0.156	0.278
4	−1.555	0.298	0.028	−1.501	0.135	7.5	−0.519	0.229	0.113	0.102	0.172	0.248

are the regression coefficients. S_i ($i=1$, 2, 3, and 4) is the coefficient for site classes I, II, III, and IV. Unlike some other works (e.g., Ghasemi et al. 2009; Soghrat et al. 2012; Ghodrati-Amiri et al. 2014), in this study, the style-of-faulting is also included in the functional form. The faulting mechanism coefficients are labeled f_s, f_{rv}, and f_{uu} for strike-slip ($F_S=1$, $F_{RV}=F_U=0$), reverse ($F_{RV}=1$, $F_S=F_U=0$) and unknown faulting ($F_U=1$, $F_S=F_{RV}=0$), respectively.

To generalize the functional form for other definitions of site classification, another model based on Vs30 is also proposed in this work. In this model (represented by Eq. 2), the site effect is studied in terms of Vs30 instead of S_i in model 1 (Eq. 1). In this functional form (model 2), γ is the regression coefficient for the site effect and V_{ref} is assumed to be equivalent to 760 m/s.

$$Log_{10}(Y) = b_1 + b_2Mw + b_3Mw^2 + (b_4 + b_5Mw)\log_{10}\sqrt{R^2 + {b_6}^2} + \gamma\log_{10}\left(V_{s30}/V_{ref}\right) + f_sF_S + f_{rv}F_{RV} + f_{uu}F_U \tag{2}$$

Table 5 Regression coefficients for vertical GMPE in model 2 using continuous Vs30

T	*b*1	*b*2	*b*3	*b*4	*b*5	*b*6		*fs*	*frv*	*fuu*	σ	τ
0	0.320	0.572	−0.038	−1.684	0.098	7.5	0.148	0.755	0.751	0.815	0.082	0.275
0.01	0.324	0.567	−0.037	−1.655	0.092	7.5	0.154	0.757	0.753	0.815	0.082	0.276
0.02	0.244	0.618	−0.040	−1.632	0.082	7.5	0.167	0.734	0.727	0.783	0.082	0.277
0.03	0.381	0.627	−0.039	−1.651	0.067	7.5	0.209	0.795	0.777	0.809	0.095	0.279
0.04	0.374	0.710	−0.046	−1.738	0.065	7.5	0.273	0.799	0.766	0.810	0.108	0.284
0.05	0.583	0.699	−0.050	−1.939	0.096	7.5	0.291	0.867	0.840	0.876	0.097	0.284
0.07	0.291	0.857	−0.062	−1.995	0.107	7.5	0.286	0.729	0.711	0.851	0.099	0.290
0.1	0.514	0.765	−0.063	−2.129	0.161	7.5	0.273	0.809	0.796	0.910	0.100	0.295
0.15	1.971	0.267	−0.045	−3.013	0.339	7.5	0.012	1.297	1.293	1.381	0.118	0.329
0.2	1.096	0.611	−0.074	−3.002	0.345	7.5	−0.075	1.046	1.004	1.046	0.145	0.294
0.25	0.115	0.795	−0.073	−2.354	0.245	7.5	−0.192	0.686	0.666	0.763	0.123	0.293
0.3	0.138	0.916	−0.097	−3.062	0.372	7.5	−0.133	0.684	0.681	0.773	0.147	0.299
0.35	−0.936	1.021	−0.074	−1.895	0.170	7.5	−0.158	0.328	0.337	0.399	0.131	0.287
0.4	−2.170	1.368	−0.085	−1.256	0.057	7.5	−0.079	−0.079	−0.077	−0.015	0.134	0.294
0.45	−2.464	1.512	−0.100	−1.468	0.096	7.5	−0.077	−0.202	−0.163	−0.100	0.145	0.295
0.5	−2.726	1.586	−0.104	−1.394	0.084	7.5	−0.091	−0.272	−0.248	−0.207	0.137	0.301
0.6	−3.346	1.710	−0.105	−1.070	0.035	7.5	−0.140	−0.454	−0.468	−0.425	0.117	0.308
0.7	−3.843	1.809	−0.107	−0.880	0.012	7.5	−0.139	−0.621	−0.629	−0.594	0.120	0.315
0.75	−3.935	1.834	−0.111	−0.959	0.033	7.5	−0.132	−0.655	−0.659	−0.621	0.120	0.316
0.8	−4.356	2.003	−0.124	−0.907	0.024	7.5	−0.122	−0.788	−0.796	−0.772	0.122	0.319
0.9	−4.701	2.085	−0.125	−0.787	0.001	7.5	−0.144	−0.896	−0.915	−0.889	0.134	0.319
1	−4.722	2.097	−0.128	−0.937	0.027	7.5	−0.169	−0.895	−0.917	−0.910	0.122	0.321
1.2	−4.434	1.854	−0.103	−0.911	0.025	7.5	−0.285	−0.791	−0.801	−0.842	0.155	0.316
1.4	−4.897	2.004	−0.112	−0.865	0.015	7.5	−0.319	−0.924	−0.972	−1.002	0.187	0.315
1.5	−4.869	1.982	−0.112	−0.930	0.026	7.5	−0.368	−0.906	−0.962	−1.002	0.205	0.311
1.6	−4.984	2.021	−0.115	−0.961	0.030	7.5	−0.411	−0.950	−0.999	−1.035	0.207	0.314
1.8	−4.379	1.635	−0.076	−0.822	0.009	7.5	−0.397	−0.757	−0.793	−0.828	0.189	0.318
2	−3.648	1.263	−0.044	−0.935	0.031	7.5	−0.355	−0.508	−0.551	−0.589	0.192	0.306
2.5	−1.920	0.327	0.037	−0.951	0.056	7.5	−0.330	0.096	0.012	−0.028	0.188	0.286
3	−1.513	0.044	0.066	−0.864	0.038	7.5	−0.373	0.226	0.147	0.115	0.161	0.271
4	−0.724	−0.467	0.113	−0.619	0.006	7.5	−0.432	0.514	0.397	0.365	0.137	0.291

4 Regression analyses and results

For development of GMPEs, two different approaches are typically applicable in the regression analyses, the two-step method and the random effects approach (Abrahamson and Youngs 1992). In this work, the regression analyses have been performed using random effects approach in which the residuals are divided into inter-event (between-event) and intra-event (within-event) terms. The regression model is given as follows:

$$\log y_{ij} = \log\mu_{ij} + \eta_i + \varepsilon_{ij}, \tag{3}$$

in which y_{ij} represents the response variable from the observed data (the geometric mean spectrum is used for the horizontal component). The μ_{ij} indicates the model prediction for data point *j* from event *i*. It is assumed that the intra-event (ε_{ij}) and inter-event (η_i) residuals are

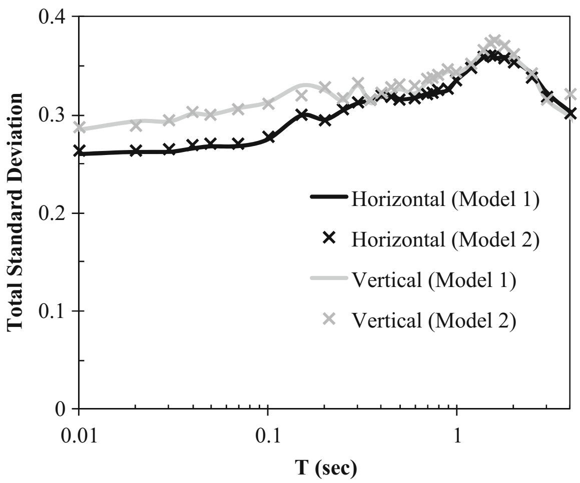

Fig. 4 Total standard deviation for models 1 and 2 in terms of period for horizontal and vertical components

independent and normally distributed with variances σ^2 and τ^2, respectively.

For a given set of regression parameters (represented by vector θ), the residuals are written as follows.

$$e_{ij}(\theta) = \log\frac{y_{ij}}{\mu_{ij}(\theta)} \tag{4}$$

A positive sign for the residuals implies under-prediction results with respect to the observed data. The total standard deviation for the residuals in each spectral period is given as

$$\sigma_T = \left(\sigma^2 + \tau^2\right)^{0.5} \tag{5}$$

Each iteration of random effects procedure requires minimization of the residual $e_{ij}(\theta)$ with respect to θ. For minimization of the residuals, the following norm proposed by Abrahamson and Youngs (1992) is used.

$$\Gamma = \left(\sum_{i=1}^{N_e}\sum_{j=1}^{N_{is}.N_T}\left[e_{ij}(\theta)\right]^2\right)^{0.5} \tag{6}$$

where N_e indicates the number of earthquake events in the analysis, N_{is} is the number of observations, and N_T is assumed as the number of discrete spectral periods. In this investigation, N_T is chosen equivalent to 31 for the periods between 0 and 4 s.

For model 1, based on Eq. 1, the regression coefficients for the median ground motion prediction and their corresponding standard deviations are given in Tables 2 and 3 for horizontal and vertical components, respectively. To stabilize the results, after some trial and error, the value of b_6 is assumed as a period-independent parameter ($b_6 = 7.5$).

In case of using model 2, the regression coefficients for the median ground motion prediction are derived separately and shown in Tables 4 and 5. Again, similar to the model 1, the b_6 coefficient is assumed equal to 7.5 as a period-independent parameter.

The total standard deviations for both horizontal and vertical components are shown in Fig. 4. The average total standard deviations in the range of period 0 to 4 s using model 1 are estimated about 0.312 and 0.326 for horizontal and vertical GMPEs, respectively. In model 2, these values are about 0.312 and 0.329 for horizontal and vertical components without significant differences comparing with model 1. These values are smaller than those resulting from some other models in the studied region. The average total standard deviation for horizontal GMPEs in this region are reported as 0.42, 0.334, and 0.328 by Motazedian (2006), Ghasemi et al. (2009), and Saffari et al. (2012), respectively.

The inter-event and intra-event residuals of the proposed models for both horizontal and vertical components of earthquakes are shown in Figs. 5, 6, 7, and 8. As shown in figures, there is not a noticeable trend between inter-event residuals and moment magnitude of earthquakes for both horizontal and vertical components. Also, according to these figures, the intra-event residuals are unbiased with respect to the moment magnitude and distance parameters. To show the residual bias in terms of distance and magnitude, average of residuals in different magnitude and distance ranges are also shown in the same figures (using cross symbol). In this case, the magnitude bin is chosen 0.5 (ΔMw) and for the distance, ΔR is selected as 25 km. A line fitting is also performed on inter-event and intra-event residuals to find the bias of the proposed model with respect to distance and magnitude parameters.

These observations show that the data and the functional forms used in this study are consistent and the models fit the data appropriately. It should be noted that the GMPEs for horizontal and vertical components of ground motion at site class IV may not be considered accurate due to the lack of sufficient data (less than 2 % of records are related to site class IV).

To investigate the suitability of the dataset used in this study, it is decided to exclude ten events without a reported moment magnitude (8 % of the records discussed earlier in this work) from the database and repeat the procedure again. Results showed no practical changes in the model prediction.

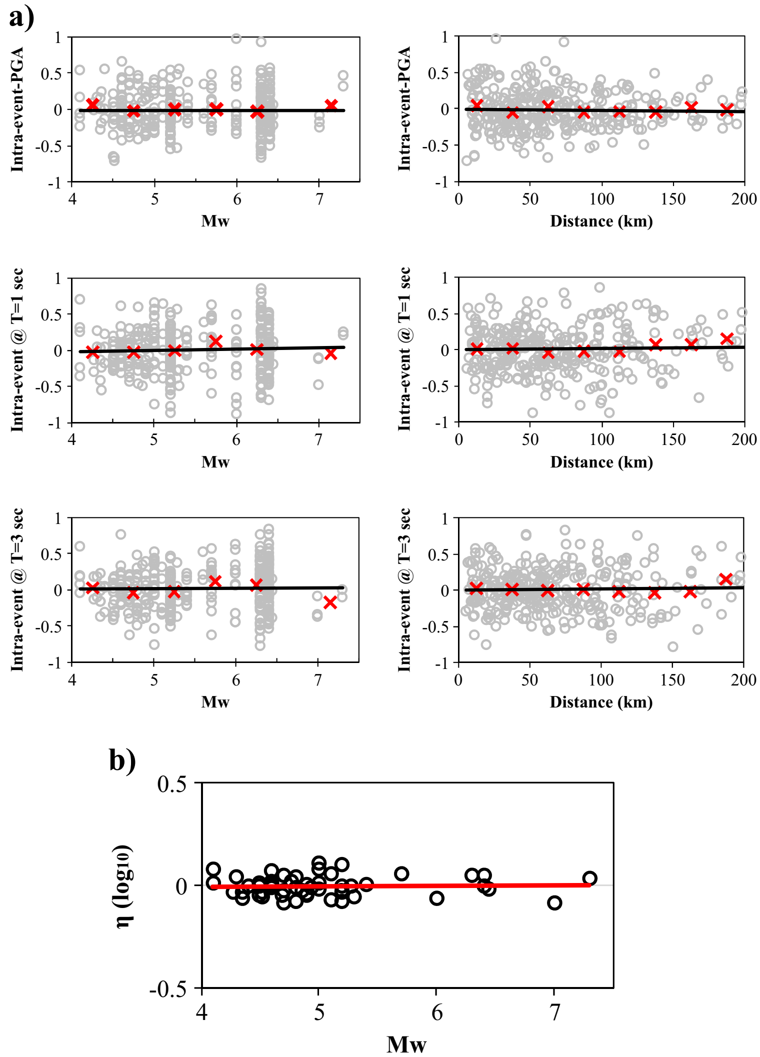

Fig. 5 The error terms for horizontal GMPEs in model 1: **a** intra-event residuals as a function of distance and magnitude and **b** inter-event residuals as a function of magnitude

Figures 9 and 10 are representing the predicted values for peak ground acceleration and PSA at periods of 0.5, 1, and 3 s versus distance. These figures are based on the moment magnitude of 6 and site class II (Vs30 is equal to 500 m/s) for both horizontal and vertical components. Model 1 and model 2 are also compared with each other in the same figures. In addition to the median values, the median plus/minus a standard deviation is also shown for the comparison. The figures show a close similarity in predicted values between the models. According to the figure, saturation of spectral amplitudes in near distances is quite similar to those reported in common literature (e.g., Campbell and Bozorgnia 2014; Boore et al. 2013; Abrahamson et al. 2014; Chiou and Youngs 2014; Idriss 2014).

Figures 9a and 10a show the observed values in case of reverse faulting for two events with the moment magnitude close to 6 in the dataset (M_w = 5.7 and 6.3). For the strike-slip faulting (shown in Figs. 9b and 10b), there is only one event with M_w = 6.0 in the dataset and therefore, the observed data and predicted values are in a better agreement. Generally speaking, it is believed that the observed values for PGA and PSAs are consistent with the predicted values.

A comparison between horizontal and vertical components of response spectra at magnitudes of 5, 6, and 7 and distances of 15, 60, and 100 km for the site class II is shown in Fig. 11. In addition to the horizontal and vertical components, the vertical to horizontal spectral ratio (V/H) is also plotted in the same figure.

Fig. 6 The error terms for vertical GMPEs in model 1: **a** intra-event residuals as a function of distance and magnitude and **b** inter-event residuals as a function of magnitude

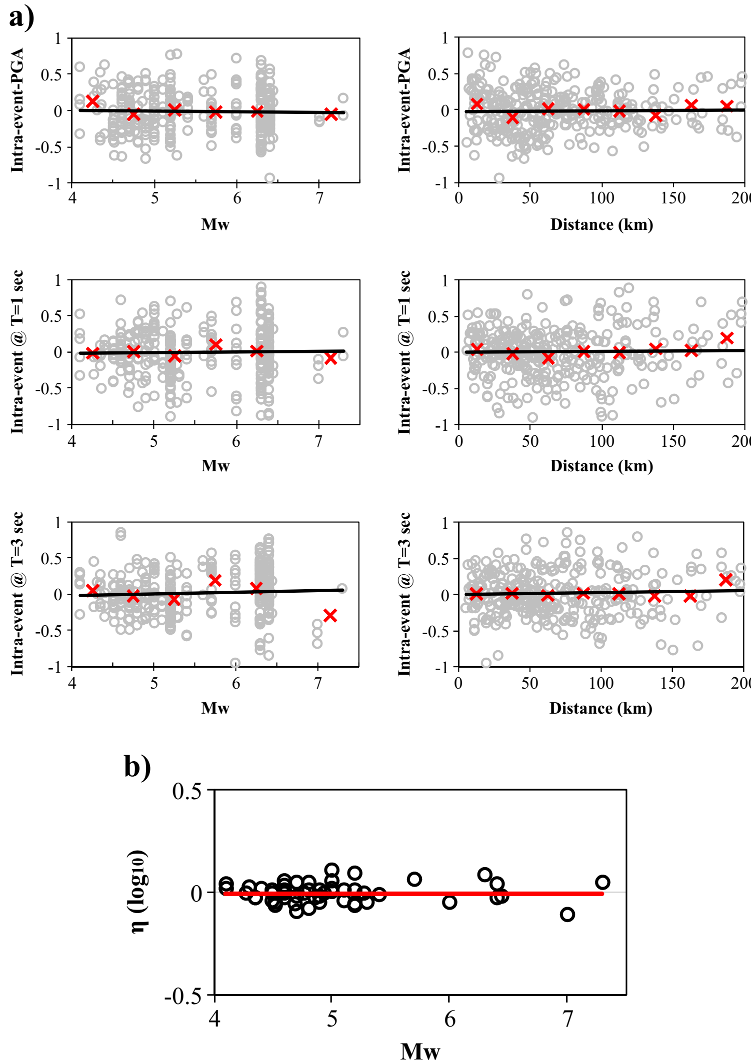

The figure shows that the spectral amplitudes decrease as the distance increases in both horizontal and vertical components. According to the figure, in the range of short periods, vertical component of spectral amplitude in near distance is larger than the horizontal one. This is in agreement with the observed data and the studies reported by Bozorgnia and Campbell (2004) as well as Kunnath et al. (2008).

As shown in the figure, the peak value in PSA is usually shifted to the shorter range of periods for the vertical component of ground motion as reported by Kunnath et al. (2008). This shift in the peak value is much more noticeable in near distances and larger magnitudes. This feature of vertical PSA is quite important in designing of buildings in the near fault regions and shows that the ratio of 2/3 recommended for scaling the horizontal spectrum to the vertical one is not credible for all ranges of spectral periods. In fact, at periods less than 0.1 s, the V/H ratio is usually greater than 2/3 (particularly for short distances). Such results are discussed by some other researchers as well (e.g., Bommer et al. 2011; Gülerce and Abrahamson 2011; Akkar et al. 2014). According to these results, vertical component of earthquake is considered important in determination of structural responses, especially in short spectral periods where the ratio of vertical-to-horizontal spectrum is high.

5 Comparisons with local and global predictive models

A comparison between the median predicted horizontal and vertical components of PSA using the proposed

Fig. 7 The error terms for horizontal GMPEs in model 2: **a** Intra-event residuals as a function of distance and magnitude and **b** inter-event residuals as a function of magnitude

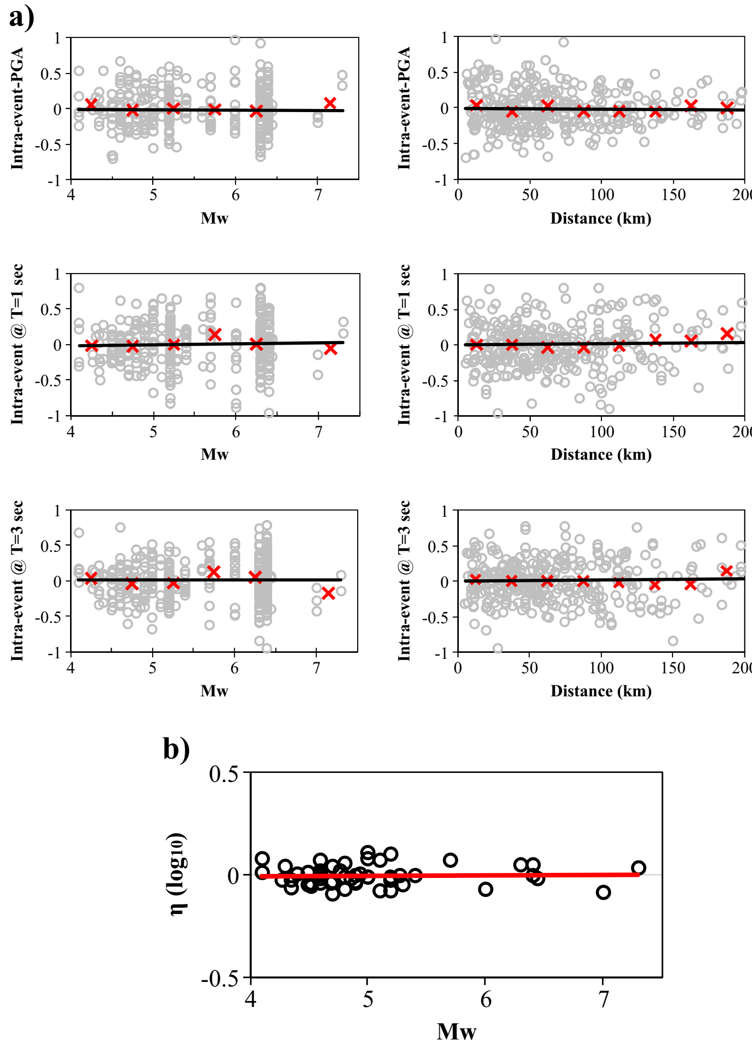

ground-motion models with those by other available GMPEs is necessary for validation of our models. Table 6 shows the characteristics of these GMPEs.

All the models prediction (including the model 1 proposed in this work) for PGA and PSA (at periods of 0.5, 1, and 3 s) in site class II with $M_w = 6$ are presented in Figs. 12 and 13 (for both horizontal and vertical components of ground motion). The figures are based on Vs30 = 500 m/s and reverse faulting, if needed.

The horizontal GMPEs developed in this study for distances less than 10 km is similar to the one reported by Soghrat et al. (2012), particularly at PGA and at T = 1 s. It should be noted that the period range of this model (Soghrat et al. 2012) for the comparison is up to 2 s, but the present study extends this range to 4 s.

For distances more than 10 km, the present model is similar to the models proposed by Soghrat et al. (2012) and Akkar and Bommer (2010) at PGA and at T = 0.5 s (low and middle periods). Also, the model is similar to the model proposed by Akkar and Bommer (2010) at T = 1 and 3 s (long periods). Although the methodologies in development of the current model and the one proposed by Soghrat et al. (2012) are quite different, the similarity between them is due to the fact that both of these models are developed using regional dataset (for northern Iran). According to Fig. 12, the local and regional GMPEs (Soghrat et al. 2012; Ghasemi et al. 2009; Akkar and Bommer 2010) are more compatible with the proposed models if they compared with

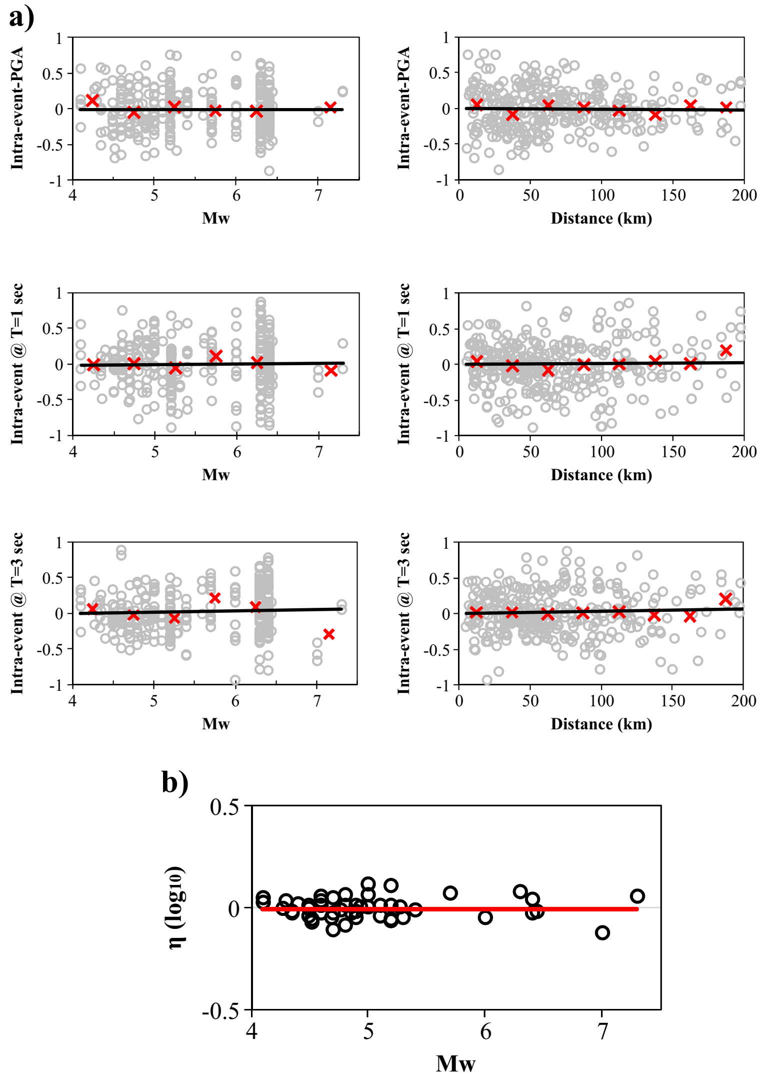

Fig. 8 The error terms for vertical GMPEs in model 2: **a** intra-event residuals as a function of distance and magnitude and **b** inter-event residuals as a function of magnitude

the models developed using worldwide data (Boore et al. 2013; Campbell and Bozorgnia 2014).

Since there are no spectral GMPEs for vertical component of earthquake in this region (only a vertical GMPE for PGA was proposed by Nowroozi 2005 in this area), having a comparison with the local GMPEs is not possible. As shown in Fig. 13 for distances less than 10 km, there is a similarity between the proposed model for PGA with the one introduced by Nowroozi (2005) and Bindi et al. (2011). At periods of 0.5 and 1 s, the proposed model is almost similar to the one developed by Bindi et al. 2010.

For distances more than 10 km, the model in current study is similar to all the models for PGA except the one by Bindi et al. (2010). At T = 0.5 and 1 s, the proposed model is similar to those of Bindi et al. (2010, 2011). In these spectral periods, the model proposed by Campbell and Bozorgnia (2003) has much higher amplitude comparing with other available models in this study due to using a dataset with a distance range less than 60 km.

Some of the differences in predictions of the models are related to the definition used for soil categories and distance parameters. The rest of the differences are presumed to be related to data density and the types of functional form and faulting mechanism.

6 Discussion and conclusions

In this study, 325 records from 55 events with moment magnitude greater than 4 and distances less

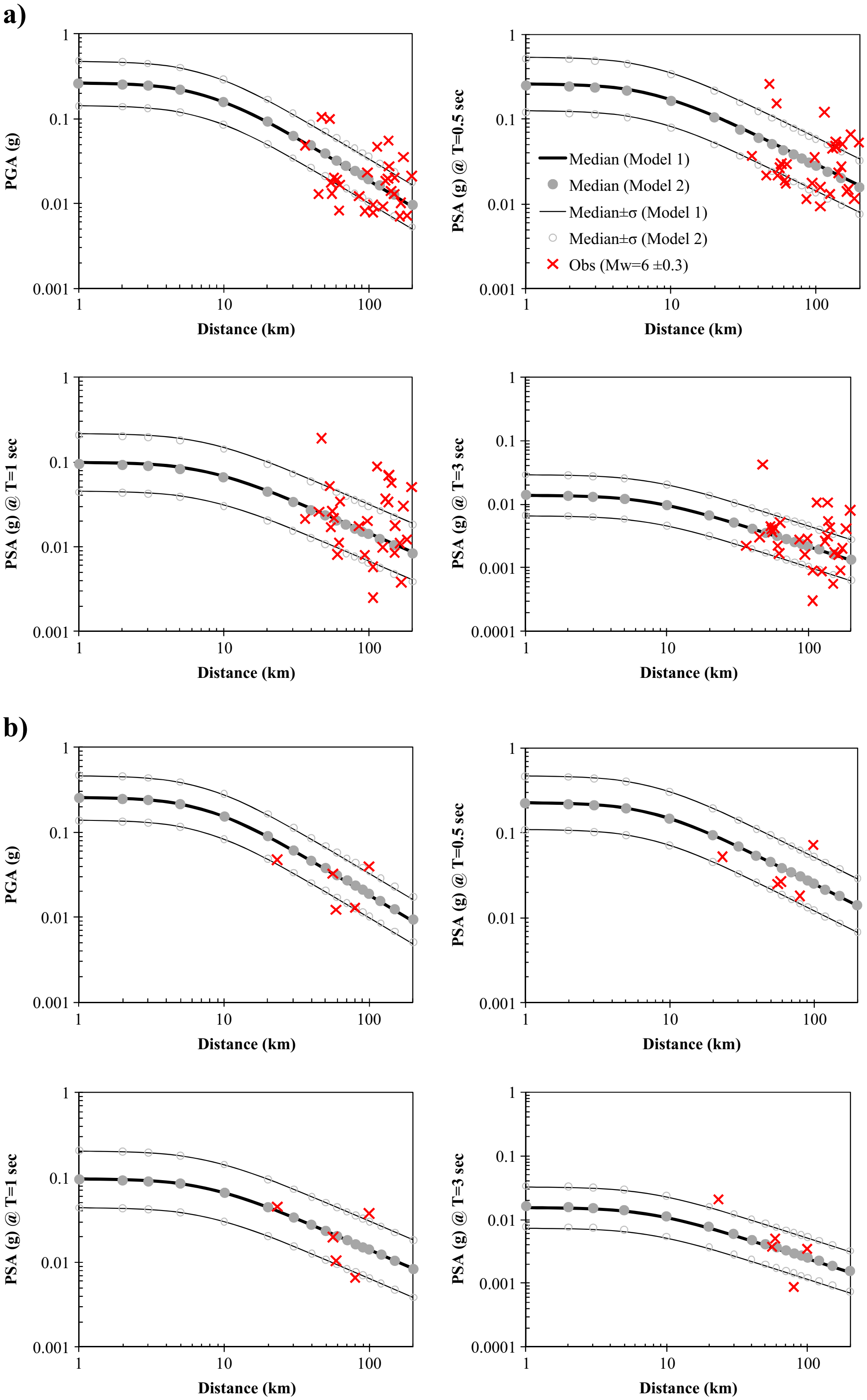

Fig. 9 Attenuation prediction of ground motion for the horizontal component assuming $M_w = 6.0$, and $SC = \text{II}$ (or Vs30 = 500 m/s) **a** reverse faulting and **b** strike-slip faulting

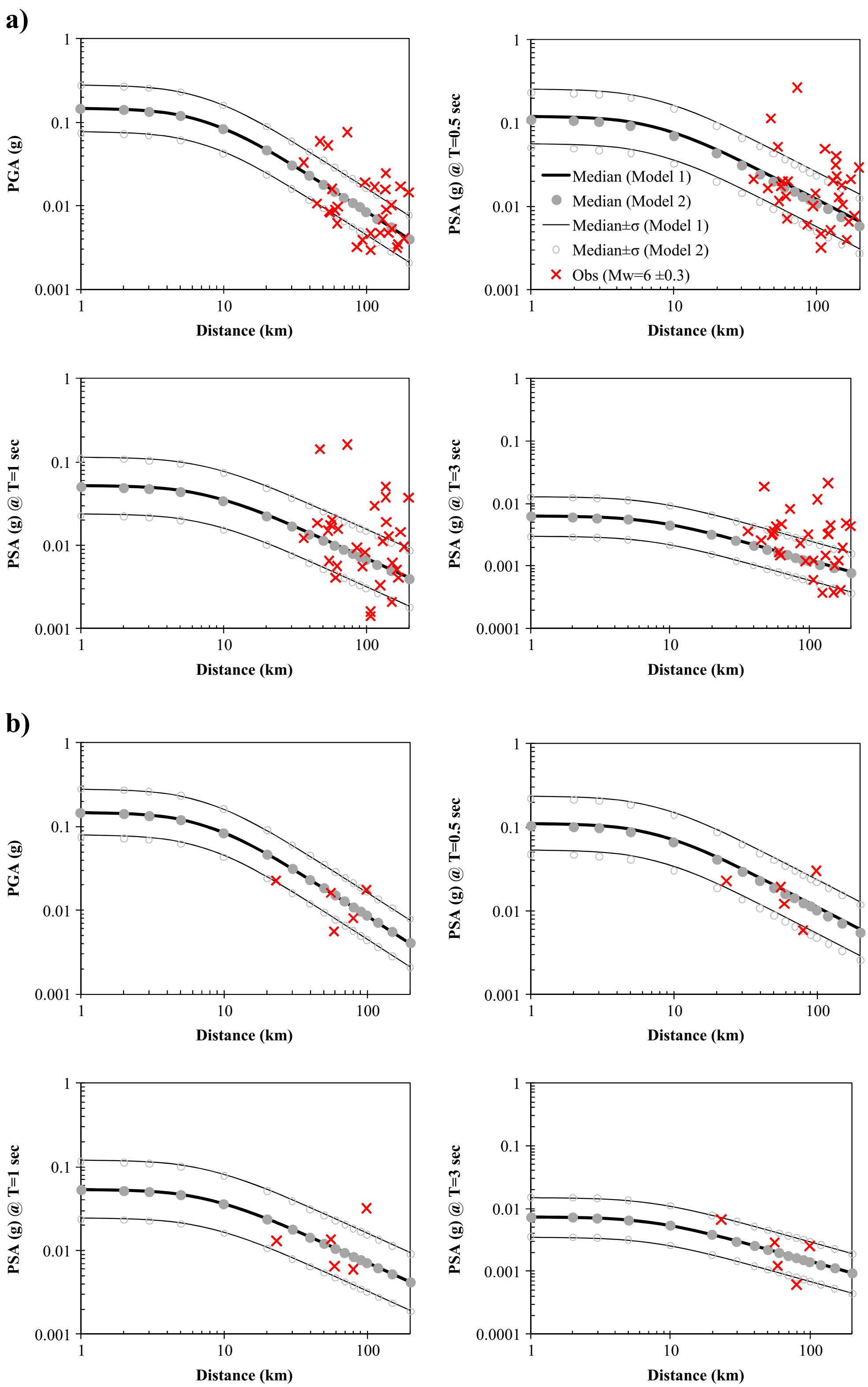

Fig. 10 Attenuation prediction of ground motion for the vertical component assuming $M_w = 6.0$, and $SC = \text{II}$ (or Vs30 = 500 m/s) **a** reverse faulting and **b** strike-slip faulting

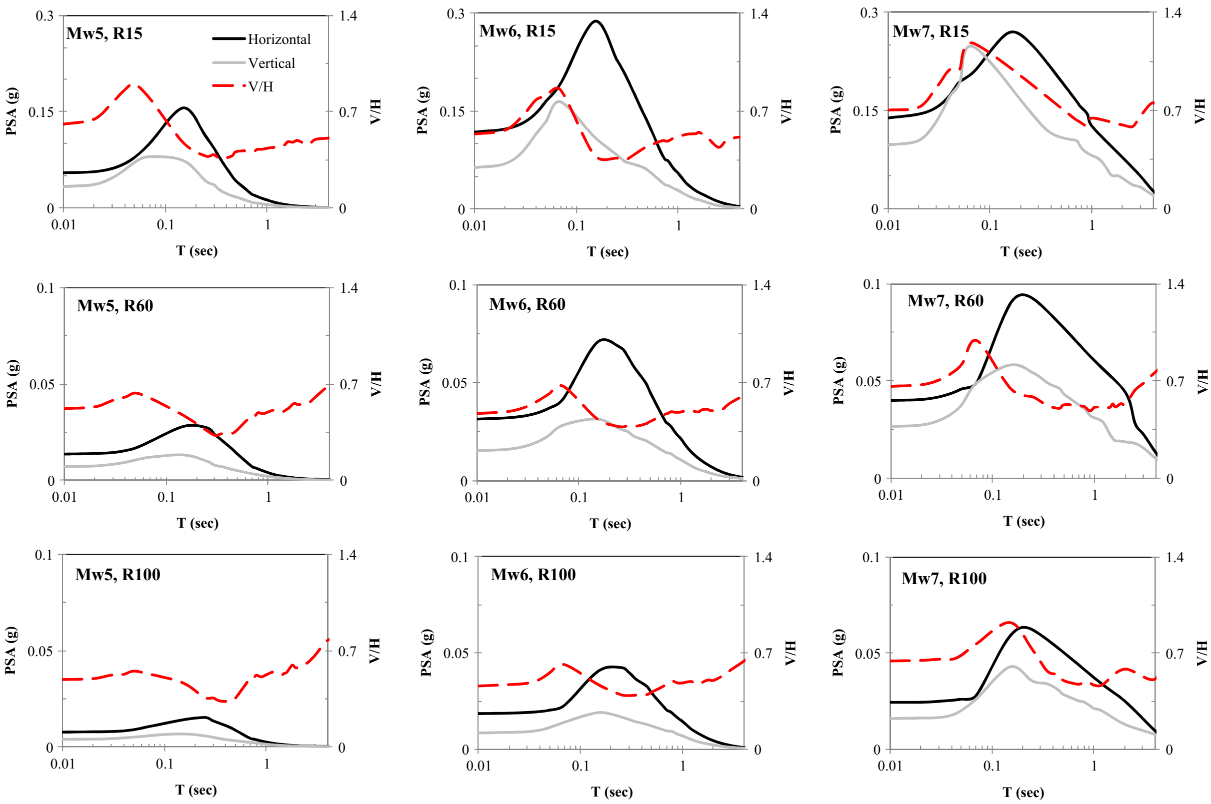

Fig. 11 Predicted horizontal and vertical PSA for $M_w = 5$, 6, 7, and distances of 15, 60, and 100 km at site class II

than 300 km have been used for development of vertical and horizontal GMPEs for northern Iran. The style-of-faulting is also included in regression analyses for both horizontal and vertical GMPEs.

Site classification in this work is based on the Iranian Code of Practice for Seismic Resistant design of Buildings (Standard 2800 2014). This site classification is similar to the one used in Eurocode 8 (2004). In addition, instead of

Table 6 Characteristics of selected GMPEs for comparison

Study	Abbreviation	Region	Component	M_w range	R[a]	R range	Range of period (s)
Soghrat et al. (2012)	Sea12	Northern Iran	Horizontal	4.9–7.4	R_{epi}	0–200	0–2
Ghasemi et al. (2009)	Gea09	Iran	Horizontal	5–7.4	R_{epi}	0–100	0.05–3
Boore et al. (2014)	BSSA14	Worldwide	Horizontal	3–7.9	R_{jb}	0–400	0–10
Campbell and Bozorgnia (2014)	CB14	Worldwide	Horizontal	3.3–8.5	R_{rup}	0–300	0–10
(Akkar and Bommer 2010)	AB10	Europe and the Middle East	Horizontal	5–7.6	R_{jb}	0–100	0–3
Nowroozi (2005)	N05	Iran	Vertical	3–7.4	R_{epi}	2–250	0
Bindi et al. (2010)	Bea10	Italy	Vertical	4–6.9	R_{jb}	0–100	0–2
Bindi et al. (2011)	Bea11	Italy	Vertical	4–6.9	R_{jb}	0–200	0–2
Campbell and Bozorgnia (2003)	CB03	Worldwide	Vertical	4.7–7.7	r_{seis}	0–60	0–4

[a] R_{jb}, R_{epi}, R_{hypo}, R_{rup}, and r_{seis} indicate closest distance to horizontal projection of rupture surface, epicentral distance, hypocentral distance, closest distance to rupture surface, and shortest distance between the recording site and the zone of the seismogenic energy release on the causative fault

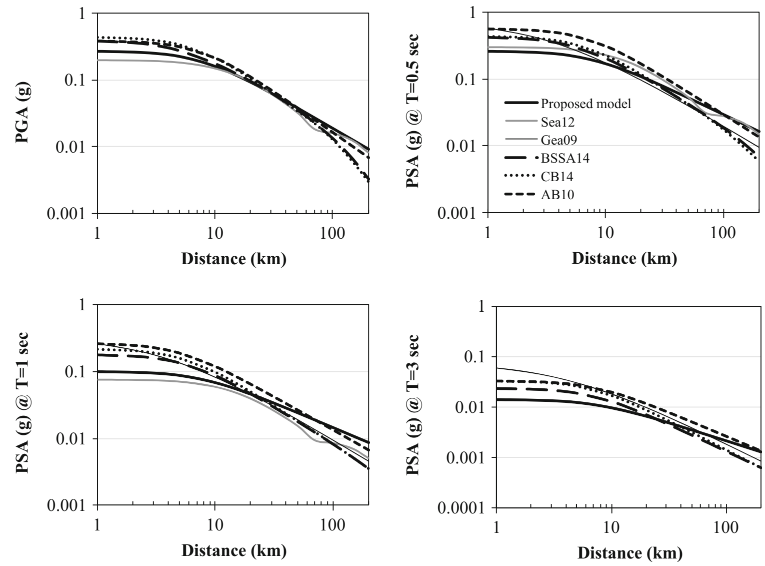

Fig. 12 Comparing all the models prediction considering $M_w = 6$, SC = II (Vs30 = 500) in case of reverse faulting for the horizontal component

using site groups (site classes I, II, III, and IV), another model for GMPEs based on using Vs30 for site effects consideration is also introduced in this work. The study shows that the predicted ground motions are in a good agreement using either approach. However, the results of regression analyses for the site classification IV in this study may be not considered reliable due to lack of records in the studied region.

The vertical GMPEs in the form of spectral amplitude proposed in this work is considered among the first attempts in development of such models in this region. The total standard deviations of proposed models for both horizontal and vertical components of ground motion represent their higher accuracy if they compare with other available local models in the studied region. The intra- and inter-event errors of these models are stable without any dependency on distance and magnitude parameters in terms of spectral periods.

Although the trends of the main features of the proposed models are similar to those reported in common literature, the spectral amplitudes of these models are not similar to other available models (due to using regional dataset).

The proposed model for the horizontal GMPE is similar to the models suggested by Soghrat et al. (2012) and Akkar and Bommer (2010). The model introduced for vertical component has a close similarity with the models

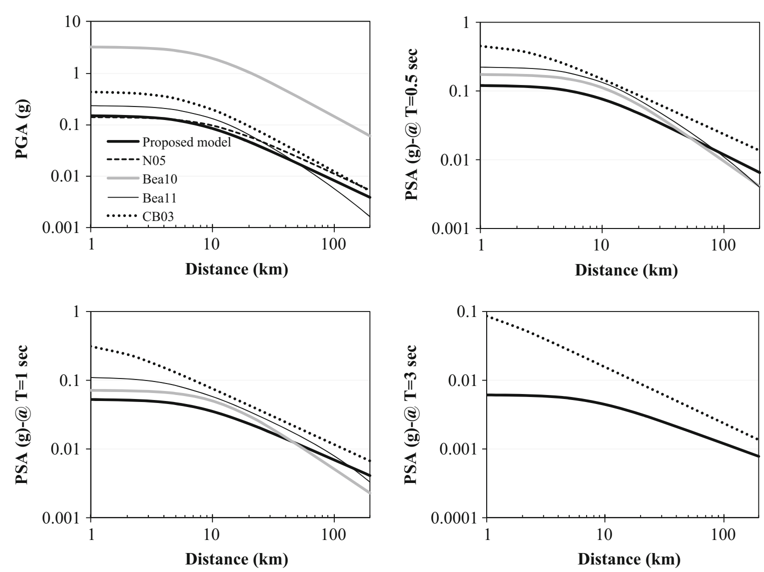

Fig. 13 Comparing all the models prediction considering $M_w = 6$, SC = II (Vs30 = 500) in case of reverse faulting for the vertical component

proposed by Bindi et al. (2011, 2011) and Nowroozi (2005) wherever a comparison was possible.

To be accurate, the proposed models may not be used for distances more than 200 km and magnitude more than 7.3 (due to insufficiency of data in this region).

Acknowledgments This project is sponsored financially by the International Institute Earthquake Engineering and Seismology (IIEES) under the grant number 618. This support is gratefully acknowledged. The authors would like to thank the Building and Housing Research Centre of Iran (BHRC) for providing the accelerographic database.

Appendix

Table 7 The list of acceleration time histories used in analyses procedure

No. of EQ	No. of rec.	Code	Station	lat_st	lon_st	Vs30 (m/s)	Distance
1	1	1353/01	Qazvin	36.26	50.00	456	98.3
1	2	1362/01	Ab-bar	36.93	48.95	691	33.7
2	3	1672	Kalaleh	37.38	55.50	375	164.0
2	4	1674	Maraveh Tappeh	37.90	55.96	538	135.6
2	5	1711	Gonbad-e-Kavoos	37.24	55.16	402	194.2
3	6	1687	Haris	38.25	47.12	530	61.0
3	7	1689/04	Nir	38.04	48.02	541	21.1
3	8	1690	Niyaraq	38.27	48.63	1512	75.5
3	9	1691	Razi	38.63	48.09	720	64.7
3	10	1695	Astara	38.42	48.87	189	100.9
3	11	1702	Germi	39.05	48.06	712	108.3
3	12	1724	Namin	38.42	48.48	1236	70.0
3	13	1725	Sarab	37.94	47.54	406	28.5
3	14	1735	Khalkhal	37.61	48.54	485	85.5
3	15	1833/02	Kariq	37.92	48.06	589	31.3
3	16	1836	Khajeh	38.15	46.59	450	105.3
3	17	1938/01	Kaleibar	38.86	47.04	850	107.0
4	18	1688	Namin	38.42	48.48	1236	69.9
4	19	1833/15	Kariq	37.92	48.06	589	17.2
5	20	1920/04	Kariq	37.92	48.06	589	19.6
5	21	1927/13	Nir	38.04	48.02	541	13.3
6	22	1905/03	Nir	38.04	48.02	541	86.1
6	23	1925	Khomarloo	39.15	47.03	921	136.4
6	24	1932	Varzaqan	38.51	46.64	475	163.4
6	25	1934	Damirchi	38.12	47.37	1241	118.0
6	26	1938/02	Kaleibar	38.86	47.04	850	127.6
6	27	1939	Aslandouz	39.45	47.40	705	125.3
6	28	2002/08	Eslam-Abad	38.13	47.94	1326	81.1
6	29	2008/01	Germi	39.05	48.06	712	53.9
6	30	2027/01	Namin	38.42	48.48	1236	32.0
6	31	2029	Niyaraq	38.27	48.63	1512	50.8
6	32	2033/01	Razi	38.63	48.09	720	36.4
6	33	2041	Ziveh	39.11	47.65	304	86.2
6	34	2046	Haris	38.25	47.12	530	130.9
6	35	2071/01	Talesh	37.80	48.90	539	107.2

Table 7 (continued)

No. of EQ	No. of rec.	Code	Station	lat_st	lon_st	Vs30 (m/s)	Distance
7	36	1919	Bile-Savar	39.36	48.32	533	75.8
7	37	2015/02	Khalkhal	37.61	48.54	485	125.2
7	38	2027/02	Namin	38.42	48.48	1236	37.0
7	39	2061/01	Astara	38.42	48.87	189	39.7
8	40	1928	Ab-bar	36.93	48.95	691	50.8
8	41	2185	Deh Jalal	36.32	48.70	748	20.9
8	42	2197	Saein Ghale	36.31	49.07	642	38.5
8	43	2198	Soltanyeh	36.44	48.80	466	10.6
8	44	2322/01	Zanjireh	38.46	45.37	919	9.1
8	45	2309/02	Marand	38.45	45.77	546	43.3
8	46	2367	Shabestar	38.18	45.71	922	45.7
8	47	2369/01	Tasooj	38.31	45.36	709	13.0
8	48	2373/01	Yekan Kahriz	38.67	45.40	738	31.0
9	49	2309/04	Marand	38.45	45.77	546	56.3
9	50	2369/04	Tasooj	38.31	45.36	709	18.7
9	51	2373/03	Yekan Kahriz	38.67	45.40	738	44.7
10	52	2203	Moalem Kelayeh	36.45	50.47	490	22.7
10	53	2209	Zavarak	36.40	50.67	489	37.0
10	54	2674/01	Jirandeh	36.70	49.80	462	59.3
11	55	2276/01	Ali Abad	36.90	54.85	562	60.0
11	56	2290/06	Astaneh	36.27	54.10	196	117.7
11	57	2295	Dibaj	36.43	54.23	526	98.0
11	58	2299	Ghomishan	37.07	54.08	322	37.8
11	59	2306	Ghalehno Kharaqan	36.63	55.07	381	96.0
11	60	2360	Incheh Borun	37.46	54.72	283	34.3
11	61	2363	Kalaleh	37.38	55.50	375	98.3
11	62	2366/01	Ramyan	37.02	55.14	827	73.4
11	63	2371	Bandar-e-Gaz	36.76	53.95	347	71.3
12	64	2276/02	Ali Abad	36.90	54.85	562	6.4
12	65	2358	Gonbad-e-Kavoos	37.24	55.16	402	40.9
12	66	2364/01	Maraveh Tappeh	37.90	55.96	538	142.1
12	67	2366/02	Ramyan	37.02	55.14	827	23.4
13	68	2400	Eslam-Abad	39.57	47.68	1326	69.3
13	69	2327/02	Bile-Savar	39.36	48.32	533	74.7
13	70	2328/02	Germi	39.05	48.06	712	110.1
14	71	2421	Qareh Aghaj	37.13	46.98	783	40.0
14	72	2422	Hashtrood	37.48	47.05	681	22.0
14	73	2431	Torkmanchay	37.58	47.39	542	22.2
15	74	2387	Gomishan	37.07	54.08	322	47.2
15	75	2389	Bandar-e-Gaz	36.76	53.95	347	37.6
15	76	2390	Dibaj	36.43	54.23	526	34.1
16	77	2557	Kerend	37.97	55.52	279	89.0
16	78	2558	Kalaleh	37.38	55.50	375	142.0
16	79	2559/02	Qapan-e-Olya	37.62	55.68	410	127.4

Table 7 (continued)

No. of EQ	No. of rec.	Code	Station	lat_st	lon_st	Vs30 (m/s)	Distance
17	80	2564	TazehKandi	39.05	47.74	461	40.2
17	81	2595	Ziveh	39.11	47.65	304	31.9
18	82	2672	Fooman	37.22	49.30	278	47.9
18	83	2673/01	Gosht	37.18	49.28	297	50.8
18	84	2677	Masooleh	37.15	48.98	956	47.4
18	85	2678	Rezvanshahr	37.55	49.12	307	11.4
18	86	2867	Koloor	37.39	48.72	860	31.9
19	87	2866	Helabad	37.94	48.42	387	57.9
19	88	2870	Hir	38.08	48.49	612	44.5
20	89	2673/02	Gosht	37.18	49.28	297	25.9
20	90	2676/03	Roodbar	36.81	49.40	595	18.6
20	91	2688	Ab-bar	36.92	48.95	691	42.3
21	92	2696	Reiskola	36.38	52.03	525	9.5
21	93	2697	Noor	36.57	52.01	178	11.9
22	94	2705/02	Jirandeh	36.70	49.78	462	17.6
22	95	2735	Moalem Kelayeh	36.45	50.47	490	66.2
22	96	2737	Nikooeyeh	36.28	49.55	1007	34.1
22	97	2760/01	Zya Abad	36.00	49.45	815	66.0
22	98	2769/01	Darsejin	36.02	49.23	636	74.2
22	99	2787/01	Bak Kandi	36.40	49.57	308	22.2
22	100	2825	Alulak	36.42	50.03	1458	29.5
22	101	2884	Razjerd	36.35	50.18	898	45.0
22	102	2885/01	Sirdan	36.65	49.18	352	51.4
22	103	2887	Zavarak	36.40	50.67	489	84.8
22	104	2786/01	Agha Baba	36.34	49.76	617	22.9
23	105	3468	Marand	38.45	45.77	546	80.7
23	106	3472	Sharafkhaneh	38.17	45.49	466	78.6
23	107	3476/01	Zanjireh	38.46	45.37	919	49.0
24	108	3295	TEHRAN 18	35.74	51.37	511	63.2
24	109	3304	TEHRAN 24	35.75	51.16	522	70.3
24	110	3306	TEHRAN 30	35.83	51.47	481	51.2
24	111	3312	TEHRAN 17	35.67	51.51	693	68.3
24	112	3315	Hashtgerd	35.96	50.68	706	88.6
24	113	3318	Taleqan	36.18	50.76	462	74.7
24	114	3321	Mard Abad	35.73	50.85	304	90.0
24	115	3323	Boomehen	35.73	51.86	696	66.2
24	116	3329	Ab-bar	36.93	48.95	691	246.0
24	117	3331	Abgarm	35.76	49.28	199	215.2
24	118	3333	Hasan Keyf	36.50	51.15	339	45.7
24	119	3334	Kahrizak	35.50	51.37	323	89.0
24	120	3336	Garmsar	35.23	52.33	817	135.1
24	121	3343	Hassan Abad	35.37	51.25	450	105.7
24	122	3347	TEHRAN 27	35.74	51.66	569	60.6
24	123	3353	Alulak	36.42	50.03	1458	140.0

Table 7 (continued)

No. of EQ	No. of rec.	Code	Station	lat_st	lon_st	Vs30 (m/s)	Distance
24	124	3354	Babolsar	36.70	52.66	187	107.2
24	125	3358	Neka	36.63	53.28	392	156.9
24	126	3361	Tonekabon	36.81	50.88	252	86.1
24	127	3367	Moalem Kelayeh	36.45	50.47	490	101.4
24	128	3368/01	Noshahr	36.65	51.49	165	41.9
24	129	3369/01	Noor	36.57	52.01	178	50.0
24	130	3371	Soltanyeh	36.44	48.80	466	250.0
24	131	3373	Roodsar	37.14	50.28	240	150.5
24	132	3374	Nozar Abad	36.80	53.25	438	160.0
24	133	3378	Jirandeh	36.70	49.80	462	166.2
24	134	3380	Khondab	34.39	49.18	466	303.1
24	135	3384	Sirdan	36.65	49.18	352	218.9
24	136	3385	Zya Abad	36.00	49.45	815	194.2
24	137	3393	Fooman	37.23	49.32	278	227.7
24	138	3398	Bandar-e-Kyashahr	37.42	49.93	184	194.2
24	139	3400	Eyvanaki	35.34	52.07	722	113.6
24	140	3403	Vahidiyeh	35.61	51.02	300	90.2
24	141	3411/02	Estalkh Posht	36.46	53.48	572	171.3
24	142	3421/02	Agha Baba	36.34	49.76	617	163.6
24	143	3422	Bak Kandi	36.40	49.57	308	180.9
24	144	3423	Qazvin1	36.26	50.00	456	142.0
24	145	3424	Kahak	36.12	49.75	686	165.5
24	146	3425	Takestan	36.07	49.70	474	170.7
24	147	3431	Babol	36.54	52.68	155	102.5
24	148	3434	Gosht	37.19	49.29	297	228.1
24	149	3437	Roodbar	36.81	49.41	595	203.0
24	150	3438	Rasht 3	37.20	49.64	334	201.2
24	151	3440	Rezvanshahr	37.55	49.14	307	259.2
24	152	3444	Razjerd	36.35	50.18	898	126.0
24	153	3445	Chandab	35.42	51.93	702	100.9
24	154	3456	Abhar	36.15	49.22	291	212.6
24	155	3457	Darsejin	36.02	49.24	636	212.5
24	156	3458	Saein Ghale	36.31	49.07	642	225.4
25	157	3365/03	Hasan Keyf	36.50	51.15	339	19.5
25	158	3368/02	Noshahr	36.65	51.49	165	21.1
25	159	3369/03	Noor	36.57	52.01	178	58.2
25	160	3370	Reiskola	36.38	52.03	525	60.6
26	161	3368/03	Noshahr	36.65	51.49	165	38.3
26	162	3369/04	Noor	36.57	52.01	178	42.1
27	163	3178	Noshahr	36.65	51.49	165	34.1
27	164	3419	Noor	36.57	52.01	178	38.2
28	165	3522	Sharafkhaneh	38.17	45.49	466	45.9
28	166	3538	Marand	38.45	45.77	546	41.1
28	167	3583/01	Tasooj	38.31	45.36	709	28.0

Table 7 (continued)

No. of EQ	No. of rec.	Code	Station	lat_st	lon_st	Vs30 (m/s)	Distance
28	168	3830/02	Zanjireh	38.46	45.37	919	12.0
29	169	3557/03	Bandar-e-Gaz	36.76	53.95	347	57.9
29	170	3568	Gomishan	37.07	54.08	322	26.4
30	171	3607	Gomishan	37.07	54.08	322	40.3
30	172	3609	Bandar-e-Gaz	36.76	53.95	347	61.2
30	173	3611	Nozar Abad	36.80	53.25	438	117.5
30	174	3612	Ali Abad	36.90	54.85	562	33.2
30	175	3614	Gonbad-e-Kavoos	37.24	55.16	402	59.8
30	176	3615	Neka	36.63	53.28	392	121.2
30	177	3618	Incheh Borun	37.46	54.72	283	47.3
30	178	3619/02	Kalaleh	37.38	55.50	375	92.8
30	179	3621/02	Ramyan	37.02	55.14	827	54.3
30	180	3622/02	Mojen	36.48	54.65	876	65.8
30	181	3624	Dibaj	36.43	54.23	526	75.1
30	182	3635	Agh Band	37.66	55.18	402	88.7
30	183	3639/05	Minoodasht1	37.23	55.37	449	76.4
30	184	3640	Qezlar	37.80	54.99	255	91.9
30	185	3642/02	Ghalehno Kharaqan	36.63	55.07	381	67.9
31	186	3920	Bandar-e-Gaz	36.76	53.95	347	81.0
31	187	3919	Gomishan	37.07	54.08	322	47.4
32	188	4206	Khalkhal	37.61	48.54	485	33.4
32	189	4207/01	Koloor	37.39	48.72	860	7.1
32	190	4209	Rezvanshahr	37.55	49.14	307	34.1
32	191	4225	Ab-bar	36.93	48.95	691	54.0
33	192	4418	Hir	38.08	48.49	612	79.3
33	193	4417	Bile-Savar	39.37	48.32	533	68.5
33	194	4419	Helabad	37.94	48.43	387	96.3
33	195	4422	Odloo	39.30	48.16	445	68.6
33	196	4424	Taleb-e-Qeshlaqi	38.40	48.21	978	55.1
33	197	4416	Astara	38.42	48.87	189	47.2
33	198	4423	Razi	38.63	48.10	720	47.3
33	199	4426	Eslam-Abad	38.13	47.94	1326	93.5
33	200	4483	Ardebil3	38.22	48.33	659	68.0
33	201	4427	Germi	39.05	48.06	712	55.2
33	202	4425	Lahrood	38.51	47.83	981	74.3
33	203	4421	Namin	38.42	48.48	1236	42.2
34	204	4467	Basmanj	38.00	46.47	564	14.6
34	205	4465	Khajeh	38.15	46.59	450	19.4
35	206	4503/01	Khajeh	38.154	46.589	450	19.1
35	207	4502/01	Basmanj	37.996	46.471	564	10.6
36	208	4502/02	Basmanj	37.996	46.471	564	10.9
36	209	4503/02	Khajeh	38.154	46.589	450	15.9
36	210	4501	Amand	38.231	46.156	743	28.6
37	211	4507	Basmanj	37.996	46.471	564	9.5

Table 7 (continued)

No. of EQ	No. of rec.	Code	Station	lat_st	lon_st	Vs30 (m/s)	Distance
37	212	4505	Khajeh	38.154	46.589	450	19.3
38	213	4562	Khalkhal	37.61	48.54	485	33.0
38	214	4561	Koloor	37.39	48.72	860	20.9
39	215	4607	Sirdan	36.65	49.19	352	47.1
39	216	4604	Ab-bar1	36.93	48.95	691	40.2
39	217	4602	Soltanyeh	36.44	48.80	466	26.4
39	218	4601	Saein Ghale	36.31	49.07	642	52.4
39	219	4606	Darsejin	36.02	49.24	636	86.8
40	220	4666	Zanjireh	38.46	45.37	919	40.9
40	221	4661	Yekan Kahriz	38.67	45.40	738	29.6
40	222	4665	Tasooj	38.31	45.36	709	52.2
40	223	4664	Shabestar	38.18	45.71	922	55.6
40	224	4663	Marand	38.45	45.77	546	25.7
41	225	5522-1	Ajab Shir	37.49	45.89	657	121.7
41	226	5523-1	Amand	38.23	46.16	743	57.0
41	227	5528-1	Basmanj	38.00	46.47	564	45.3
41	228	5532-1	Damirchi	38.12	47.37	1241	54.3
41	229	5538-1	Hadi Shahr	38.84	45.66	475	115.2
41	230	5540-1	Haris	38.25	47.12	530	28.7
41	231	5545-1	Kaleibar	38.87	47.04	850	65.7
41	232	5547-1	Khajeh	38.15	46.59	450	25.3
41	233	5551-1	Lahrood	38.51	47.83	981	92.1
41	234	5554-1	Marand	38.45	45.77	546	90.8
41	235	5556-1	Nazarkahrizi	37.35	46.75	519	107.0
41	236	5564-1	Sarab	37.94	47.54	406	77.2
41	237	5565-1	Sharabiyan	37.89	47.10	484	54.0
41	238	5567-1	Shabestar	38.18	45.71	922	96.6
41	239	5570-1	Soofiyan	38.28	45.98	707	71.7
41	240	5575-1	Tasooj	38.31	45.36	709	125.7
41	241	5576-1	Torkmanchay	37.58	47.39	542	96.5
41	242	5579-1	Varzaqan	38.51	46.64	475	26.0
41	243	5580-1	Yekan Kahriz	38.67	45.40	738	128.2
41	244	5581-1	Zanjireh	38.46	45.37	919	126.2
41	245	5601-1	Khomarloo	39.15	47.03	921	96.0
41	246	5604-1	Ziveh	39.11	47.65	304	115.9
42	247	5522-2	Ajab Shir	37.49	45.89	657	129.6
42	248	5523-2	Amand	38.23	46.16	743	60.3
42	249	5525	Astara	38.42	48.87	189	179.3
42	250	5527	Azarshahr	37.77	45.97	660	101.4
42	251	5528-2	Basmanj	38.00	46.47	564	53.5
42	252	5532-3	Damirchi	38.12	47.37	1241	57.4
42	253	5537	Germi	39.05	48.06	712	130.3
42	254	5538-2	Hadi Shahr	38.84	45.66	475	111.8
42	255	5539-2	Hashtrood	37.48	47.05	681	104.4

Table 7 (continued)

No. of EQ	No. of rec.	Code	Station	lat_st	lon_st	Vs30 (m/s)	Distance
42	256	5540-3	Haris	38.25	47.12	530	31.3
42	257	5542	Helabad	37.94	48.43	387	149.9
42	258	5543	Talesh	37.84	48.90	539	192.6
42	259	5545-3	Kaleibar	38.87	47.04	850	56.5
42	260	5547-3	Khajeh	38.15	46.59	450	33.2
42	261	5548	Kariq	37.92	48.06	589	121.4
42	262	5549	Koraiem	37.96	48.24	787	133.7
42	263	5551-2	Lahrood	38.51	47.83	981	89.1
42	264	5554-2	Marand	38.45	45.77	546	90.9
42	265	5555	Namin	38.42	48.48	1236	145.1
42	266	5556-2	Nazarkahrizi	37.35	46.75	519	116.4
42	267	5559	Nir	38.03	47.99	541	110.7
42	268	5560	Odloo	39.30	48.16	445	154.2
42	269	5564-2	Sarab	37.94	47.54	406	81.6
42	270	5565-2	Sharabiyan	37.89	47.10	484	61.8
42	271	5566-2	Sharafkhaneh	38.17	45.49	466	118.5
42	272	5567-2	Shabestar	38.18	45.71	922	99.6
42	273	5570-2	Soofiyan	38.28	45.98	707	73.8
42	274	5575-2	Tasooj	38.31	45.36	709	127.2
42	275	5576-2	Torkmanchay	37.58	47.39	542	103.9
42	276	5577-2	Tikmedash	37.73	46.95	442	74.8
42	277	5578	Taleb-e-Qeshlaqi	38.40	48.21	978	121.4
42	278	5579-4	Varzaqan	38.51	46.64	475	19.7
42	279	5580-2	Yekan Kahriz	38.67	45.40	738	126.7
42	280	5581-2	Zanjireh	38.46	45.37	919	126.5
42	281	5600	Eslam-Abad	38.13	47.94	1326	103.2
42	282	5601-2	Khomarloo	39.15	47.03	921	86.6
42	283	5604-2	Ziveh	39.11	47.65	304	108.0
43	284	5532/02	Damirchi	38.12	47.37	1241	60.6
43	285	5540/02	Haris	38.25	47.12	530	34.4
43	286	5545/02	Kaleibar	38.87	47.04	850	55.5
43	287	5547/02	Khajeh	38.15	46.59	450	33.5
43	288	5579/02	Varzaqan	38.51	46.64	475	16.5
44	289	5547/04	Khajeh	38.15	46.59	450	28.7
44	290	5579/20	Varzaqan	38.51	46.64	475	12.8
45	291	5532/05	Damirchi	38.12	47.37	1241	60.4
45	292	5547/06	Khajeh	38.15	46.59	450	35.5
45	293	5593/01	Haris	38.25	47.12	530	34.3
45	294	5605/01	Kaleibar	38.87	47.04	850	53.5
46	295	5532/06	Damirchi	38.12	47.37	1241	67.1
46	296	5547/07	Khajeh	38.15	46.59	450	36.5
46	297	5593/02	Haris	38.25	47.12	530	41.0
46	298	5605/02	Kaleibar	38.87	47.04	850	52.6
47	299	5532/07	Damirchi	38.12	47.37	1241	61.6

Table 7 (continued)

No. of EQ	No. of rec.	Code	Station	lat_st	lon_st	Vs30 (m/s)	Distance
47	300	5547/09	Khajeh	38.15	46.59	450	25.1
47	301	5604/03	Ziveh	39.11	47.65	304	116.6
47	302	5605/04	Kaleibar	38.87	47.04	850	63.8
47	303	5639/03	TazehKandi	39.05	47.74	461	117.3
48	304	5579/19	Varzaqan	38.51	46.64	475	10.9
48	305	5608/02	Khajeh	38.15	46.59	450	30.7
49	306	5589/07	Varzaqan	38.51	46.64	475	14.8
49	307	5593/05	Haris	38.25	47.12	530	39.2
49	308	5595	Basmanj	38.00	46.47	564	63.7
49	309	5605/05	Kaleibar	38.87	47.04	850	45.4
49	310	5608/04	Khajeh	38.15	46.59	450	43.4
49	311	5678	Hadi Shahr	38.84	45.66	475	106.6
50	312	5589/08	Varzaqan	38.51	46.64	475	8.2
50	313	5608/05	Khajeh	38.15	46.59	450	32.5
50	314	5658	Haris	38.25	47.12	530	44.3
51	315	5589/12	Varzaqan	38.51	46.64	475	9.8
51	316	5608/06	Khajeh	38.15	46.59	450	36.0
52	317	5589/16	Varzaqan	38.51	46.64	475	10.9
52	318	5608/07	Khajeh	38.15	46.59	450	29.1
53	319	5667/13	Varzaqan	38.51	46.64	475	9.9
53	320	5679/02	Khajeh	38.15	46.59	450	29.6
54	321	5674/02	Varzaqan	38.51	46.64	475	5.3
54	322	5679/03	Khajeh	38.15	46.59	450	34.5
56	323	5670	Haris	38.25	47.12	530	57.0
56	324	5672	Kaleibar	38.87	47.04	850	65.0
56	325	5674/05	Varzaqan	38.51	46.64	475	12.2

References

Abrahamson N, Youngs R (1992) Short notes. Bull Seism Soc Am 82(1):505–510

Abrahamson NA, Silva WJ, Kamai R (2014) Summary of the ASK14 ground motion relation for active crustal regions. Earthq Spectra 30(3):1025–1055

Akkar S, Bommer JJ (2007) Empirical prediction equations for peak ground velocity derived from strong-motion records from Europe and the Middle East. Bull Seism Soc Am 97(2):511–530

Akkar S, Bommer JJ (2010) Empirical equations for the prediction of PGA, PGV, and spectral accelerations in Europe, the Mediterranean region, and the Middle East. Seismol Res Lett 81(2):195–206

Akkar S, Sandıkkaya MA, Ay BÖ (2014) Compatible ground-motion prediction equations for damping scaling factors and vertical-to-horizontal spectral amplitude ratios for the Broader Europe Region. Bull Earthq Eng 12:517–547

Ambraseys N, Douglas J (2003) Near-field horizontal and vertical earthquake ground motions. Soil Dyn Earthq Eng 23(1):1–18

Ansari A, Noorzad A, Zafarani H, Vahidifard H (2010) Correction of highly noisy strong motion records using a modified wavelet de-noising method. Soil Dyn Earthq Eng 30(11):1168–1181

ASCE 41 (2013) Seismic Rehabilitation of Existing Buildings. American Society of Civil Engineers (ASCE) Publications

Bindi D, Luzi L, Massa M, Pacor F (2010) Horizontal and vertical ground motion prediction equations derived from the Italian Accelerometric Archive (ITACA). Bull Earthq Eng 8(5):1209–1230

Bindi D, Pacor F, Luzi L, Puglia R, Massa M, Ameri G, Paolucci R (2011) Ground motion prediction equations derived from the Italian strong motion database. Bull Earthq Eng 9(6):1899–1920

Bommer JJ, Akkar S, Kale Ö (2011) A model for vertical-to-horizontal response spectral ratios for Europe and the Middle East. Bull Seism Soc Am 101(4):1783–1806

Boore DM, Stewart JP, Seyhan E, Atkinson GM (2013) NGA-West 2 equations for predicting PGA, PGV, and 5%-Damped PSA for shallow crustal earthquakes., Earthq Spectra

Bozorgnia Y, Campbell KW (2004) The vertical-to-horizontal response spectral ratio and tentative procedures for developing simplified V/H and vertical design spectra. J Earthq Eng 8(2):175–207

Button MR, Cronin CJ, Mayes RL (2002) Effect of vertical motions on seismic response of highway bridges. J Struct Eng 128(12):1551–1564

Campbell KW, Bozorgnia Y (2003) Updated near-source ground-motion (attenuation) relations for the horizontal and vertical components of peak ground acceleration and acceleration response spectra. Bull Seism Soc Am 93(1):314–331

Campbell KW, Bozorgnia Y (2014) NGA-West2 Ground Motion Model for the Average Horizontal Components of PGA, PGV, and 5%-Damped Linear Acceleration Response Spectra., Earthq Spectra

Chiou BSJ, Youngs RR (2014) Update of the Chiou and Youngs NGA model for the average horizontal component of peak ground motion and response spectra. Earthq Spectra 30(3):1117–1153

Elnashai A, Papazoglou A (1997) Procedure and spectra for analysis of RC structures subjected to strong vertical earthquake loads. J Earthq Eng 1(01):121–155

Eurocode 8 (2004) Eurocode 8: design of structures for earthquake resistance. Part 1: 1998-1991

FEMA 356 (2000) Commentary for the seismic rehabilitation of buildings

FEMA P-750 (2009) NEHRP recommended seismic provisions for new buildings and other structures. Federal Emergency Management Agency, Washington, DC

Ghasemi H, Zare M, Fukushima Y, Koketsu K (2009) An empirical spectral ground-motion model for Iran. J Seism 13(4):499–515

Ghodrati-Amiri GR, Khorasani M, Hessabi RM, Amrei SR (2009) Ground-motion prediction equations of spectral ordinates and Arias intensity for Iran. J Earthq Eng 14(1):1–29

Ghodrati-Amiri GR, Amiri MS, Tabrizian Z (2014) Ground motion prediction equations (GMPEs) for elastic response spectra in the Iranian plateau using Gene Expression Programming (GEP). J Intell Fuzzy Syst 26(6):2825–2839

Gülerce Z, Abrahamson NA (2011) Site-specific design spectra for vertical ground motion. Earthq Spectra 27(4):1023–1047

Halldorsson B, Papageorgiou AS (2005) Calibration of the specific barrier model to earthquakes of different tectonic regions. Bull Seism Soc Am 95(4):1276–1300

Idriss IM (2014) An NGA-West2 empirical model for estimating the horizontal spectral values generated by shallow crustal earthquakes. Earthq Spectra 30(3):1155–1177

Kunnath SK, Erduran E, Chai Y, Yashinsky M (2008) Effect of near-fault vertical ground motions on seismic response of highway overcrossings. J Bridge Eng 13(3):282–290

Mirzaei N, Mengtan G, Yuntai C (1998) Seismic source regionalization for seismic zoning of Iran: major seismotectonic provinces. J Earthq Predict Res 7:465–495

Motazedian D (2006) Region-specific key seismic parameters for earthquakes in Northern Iran. Bull Seism Soc Am 96(4A):1383–1395

Nowroozi AA (2005) Attenuation relations for peak horizontal and vertical accelerations of earthquake ground motion in Iran: a preliminary analysis. J Seismol Earthq Eng 7(2):109–128

Palaskas M, He L, Chegini M (1996) Vertical seismic forces on elevated concrete slabs. Pract Period Struct Des Constr 1(3):88–90

Saadeghvaziri MA, Foutch D (1991) Dynamic behaviour of R/C highway bridges under the combined effect of vertical and horizontal earthquake motions. Earthq Eng Struct Dyn 20(6):535–549

Saffari H, Kuwata Y, Takada S, Mahdavian A (2012) Updated PGA, PGV, and spectral acceleration attenuation relations for Iran. Earthq Spectra 28(1):257–276

Shahvar MP, Zare M, Castellaro S (2013) A unified seismic catalog for the Iranian plateau (1900–2011). Seismol Res Lett 84(2):233–249

Shakib H, Fuladgar A (2003) Response of pure-friction sliding structures to three components of earthquake excitation. Comput Struct 81(4):189–196

Sinaiean F (2006) A study on the strong ground motions in Iran (from catalog to attenuation relationship). Dissertation, International Institute of Earthquake Engineering and Seismology (IIEES)

Soghrat MR, Khaji N, Zafarani H (2012) Simulation of strong ground motion in northern Iran using the specific barrier model. Geophys J Int 188(2):645–679

Soghrat MR, Ziyaeifar M (2016) A Predictive Equation for Vertical-to-Horizontal Response Spectral Ratios in Northern Iran. Bull Seism Soc Am 106(1):123–140

Standard 2800 (2014) Iranian Code of Practice for Seismic Resistant Design of Buildings, 4th edition

Yu CP, Broekhuizen DS, Roesset JM (1997) Effect of vertical ground motion on bridge deck response. Technical Report NCEER, US Nacional Center for Earthquake Engineering Research (NCEER). Jpn Int Cent Disaster Mitig Eng (INCEDE) 97:249–263

Zafarani H, Soghrat MR (2012) Simulation of ground motion in the Zagros Region of Iran using the specific barrier model and the stochastic method. Bull Seism Soc Am 102(5):2031–2045